EXPERIMENTAL ANALYSIS OF CURVED RC BEAMS STRENGTHENED WITH CARBON FIBRE FOR FLEXURAL AND SHEAR CAPACITY ENHANCEMENT

Ruwan Pathirana Dasith Sithira Premalal

(168920N)

Degree of Master of Science

Department of Civil Engineering

University of Moratuwa

Sri Lanka

January 2022

EXPERIMENTAL ANALYSIS OF CURVED RC BEAMS STRENGTHENED WITH CARBON FIBRE FOR FLEXURAL AND SHEAR CAPACITY ENHANCEMENT

Ruwan Pathirana Dasith Sithira Premalal

(168920N)

Thesis submitted in partial fulfilment of the requirements for the degree Master of Science in Civil Engineering

Department of Civil Engineering

University of Moratuwa
Sri Lanka

January 2022

DECLARATION

I declare that this is my work and this thesis does not incorporate without acknowledgement any material previously submitted for a Degree or Diploma in any other University or institute of higher learning and to the best of my knowledge and belief it does not contain any material previously published or written by another person except where the acknowledgement is made in the text.

Also, I hereby grant to the University of Moratuwa the non-exclusive right to reproduce and distribute the thesis, in whole or in part in print, electronic or other media. I retain the right to use this content in whole or part in future works (such as articles or books).

Signature: Date:

The above candidate has carried out research for the Masters under my supervision

Name of the supervisor: Prof. (Mrs.) J.C.P.H. Gamage

Signature of the supervisor: Date:

ACKNOWLEDGEMENT

I would like to express my heartfelt gratitude to my research supervisor **Prof. (Mrs.) J.C.P.H. Gamage**, Senior Lecturer at the Department of Civil Engineering, University of Moratuwa for her continuous guidance and support extended throughout my research study period. The motivation provided by her held me to modify relevant parts effectively and to be inline with the time schedule to finish.

Next, I am thankful to the technical staff of Structural Testing and Building Materials Laboratory of the University of Moratuwa for their assistance and support extended during the experimental work.

Then I would like to thank my batch mates of MSc. Degree in Structural engineering 2016/2017, N.R.D. Senarathne and K.R.T.H. Indrachapa for immense support provided to me during beam casting and testing stages.

In addition, the overall arrangement of the research proceedings by Dr. H.M.Y.C. Mallikarachchi, Coordinator, MSc. in Structural Engineering is greatly appreciated. Also the assistance and encouragement given by Eng. S.D.G.L.Jayatilaka and Eng. N.D. Amarasinghe, Ceylon Electricity Board (CEB) to continue my research work during this period of 24 months immensely helped me to complete this research, parallel to work at CEB.

R. P. D. S. Premalal

MSc. Degree in Structural Engineering

Department of Civil Engineering

University of Moratuwa

31.01.2022

ABSTRACT

Among the concrete strengthening applications, Carbon Fibre Reinforced Polymer (CFRP) systems offer better mechanical properties than other alternatives, such as stronger tensile strength, stiffness, and durability. Most of the studies have been focused on strengthening or retrofitting straight Reinforced Concrete (RC) beams using CFRP, fewer on the horizontally curved out of plane loaded RC beams, which are present in novel featured structures worldwide. In contrast to straight beams, the curved beam behaviour possess combined effect of bending, torsion and shear where CFRP application requires a careful selection based on the intended capacity enhancement.

The experimental program includes total 6 nos. of RC beam specimens of fixed curvature casted, 2 beams weak under shear and 2 beams weak under flexure and their control beams. The CFRP strengthening was applied as relevant to evaluate the effectiveness of flexural and shear enhancement. The NSM CFRP plate application and end anchored NSM CFRP for flexure strengthening along with $45^0/135^0$ oriented CFRP fabrics at beam sides and increased area of fabric for shear strengthening was focused. The specimens were tested using four point bending test and the ultimate failure load, crack patterns, failure modes and deflection was observed.

The experimental results under flexure concluded that NSM CFRP enhance flexural strength according to the initial cracking load observations. Where end anchored CFRP fabric provided it contribute to additional flexure strength and reduce overall deflection by 23%. Ultimate load carrying capacity of NSM CFRP retrofitted beams were enhanced by 12.1% and 8.4% for respective application. NSM CFRP retrofitted beams showed, lesser crack density and widths. Propagation of the crack which was in the direction of NSM CFRP plate corners is restrained with the use of end anchored CFRP, although its effect over shear capacity enhancement is insignificant. The experimental flexural enhancements are 28.8% and 29.3% less than the theoretically predicted values by ACI 440.2R-17 guide, respectively for NSM CFRP only and end anchored beams, which may have occurred due to the contribution of additionally induced torsional stresses.

The experimental results under shear concluded that ultimate load carrying capacity of shear retrofitted beams were enhanced by 20 % and 30%. The influence of CFRP retrofitting is higher when the CFRP application area is increased at inner shear span. The experimental shear enhancements are 35.4% and 20.3% less than the theoretically predicted values by ACI 440.2R-17 guide, respectively for side laminated and extra side laminated beams. The intermediate debonding and induced additional torsional stresses may have caused this capacity reduction.

Table of Contents

List of Figures

List of Tables

CHAPTER 1: INTRODUCTION

1.1 Background

Fibre-reinforced polymer (FRP) is a type of composite material, consists of continuous high strength fibres of materials in particular carbon, glass or steel wires. These fibres are embedded in a formation of polymer matrix. The fibres act as the main reinforcing elements of the composite. Function of a binder is performed by the polymer matrix (epoxy resins), which protects the fibres and as well as transfers loads to and between the reinforcing elements. The resins and fibres in a FRP system are characteristically established as a single system based on materials and the structural testing. It is not permitted to mix or substitute a constituent from one FRP system with a constituent from any other, as this can create negative impact on the cured system's properties.

The use of FRP composites for structural strengthening has expanded in the recent years worldwide. During this period of development, FRP composites have revealed its applicability as a mainstream construction material. Consequently, the use of FRP in strengthening and retrofitting requirements has gained more popularity among professionals nowadays over conventional structural strengthening techniques like fixing of supplemental steel frames and other elements. For secondary concrete strengthening applications, carbon fibre-based FRP (CFRP) systems are the most frequent. Carbon exhibit better mechanical properties than glass fibre-based systems, such as stronger tensile strength, stiffness, and durability.

Curved structural beam elements applications are popularly seen in modern structures like curved roof arches, elevated highway ramps, reservoirs, curved buildings floors and balconies. According to the direction of loading in vertical or horizontal plane, the behaviour and failure modes encountered differ. Vertically curved beams have dominant axial load transfer which depends on the ultimate compressive strength of the concrete. In horizontally curved out-of-plane beam loaded vertically, torsional stresses are created along with flexural and shear stresses. The torsional stresses affect to reduce the shear capacity making the beam vulnerable to fail under shear. The structural integrity of vertically curved beams are higher compared to horizontally curved and straight beams.

FRP are widely used for curve beam retrofitting, where research areas are higher for vertically concaved structural beams. The debonding, rupture, anchorage end failure can be often observed in such experimental studies. Prior to FRP installation, strengthening requirement of existing structural element can involve complex evaluation of history, structural design and detailing processes, requiring a sound consideration of the condition of the existing structure together with the materials used to repair the damaged structure. Understanding what FRP is and the benefits it provides, as well as its limitations, can help decide its viability for a strengthening project.

A dry fabric formed of carbon or glass material is saturated with epoxy and attached to a primed concrete substrate in the wet lay-up procedure. It can be used to construct FRP composites on-site. Once cured, the it acts as an externally bonded fibre reinforcing system, becoming an integral component of the structural member. FRP composites can be configured upon usage, prefabricated in a specific manufacturing facility. The material is pultruded into various shapes or profiles, such as rods, bars and plates for use in reinforcing applications.

The straight beam retrofitting applications of FRP is abundantly in use due to ease of application and the enhancement gained in cracked structural elements. FRP fabric is available in fabric like unidirectional continuous sheets on rolls which can be simply adjusted to match any geometrical profile and can be wrapped around practically any shape. The fabrics made of fibre can be bonded to the side of tension of structural parts (beams or slabs or webs) (Figure 1-a) to offer additional tensile reinforcement, wrapped over the webs of joists or beams to enhance their shear strength and as seen on Figure 1-(b) wrapped around columns to improve ductility and energy dissipation behaviour.

(a) wrapped over the webs of beams (b) wrapped around columns

Figure 1: Different uses of CFRP wrapping

A primer that penetrates the concrete substrate and improves the system's bond may be used in the adhesive solutions used to enhance the bonding between FRP and the concrete substrate. If minor holes exist in the surface, epoxy putty need to fill into the substrate and create a even surface for the FRP to adhere to a saturating resin that is used to impregnate and adhere fabric to a prepared the substrate and followed by a protective coating in order to safeguard the bonded FRP from potentially detrimental environmental, chemical and mechanical effects. Exposure to ultraviolet radiation damages most epoxies used in FRP strengthening systems, however, such systems are possible to be preserved using acrylic, cementitious coatings or other forms of coatings.

Repairing structurally degraded reinforced concrete structures is required when the structural part no longer provides adequate overloading, strength or serviceability. Because of the high performance of FRP laminates, field application of retrofitting by epoxy-bonded FRP laminates is currently acknowledged as an effective and convenient approach through several research worldwide. In contrast to the case for use of CFRP sheets or other form for the repair of load-damaged or initially cracked RC beams, several experimental studies have focused on the member strengthening. However, in view of the research literature on out of plane loaded curved beam retrofitting experiments, the effective optimization of shear and flexural capacity using FRP need further experiments and research to evaluate the degree of enhancement.

1.2 Objectives of the Research

- To conduct an experimental program to determine the behaviour of CFRP strengthened out-of-plane curved RC beam subjected to flexure and the effect of different applications of CFRP strengthening for flexure.
- To conduct an experimental program to determine the behaviour of CFRP strengthened out-of-plane curved RC beam when subjected to fail in shear and the effect of different applications of CFRP strengthening for shear.
- To conduct a theoretical prediction of load capacities under bending and shear of the CFRP strengthened out-of-plane curved RC beams and comparison with experimental results.

- To propose conclusions on the effectiveness of different applications of CFRP flexure retrofitting to its capacity, failure mode, cracking and deflection of the out of plane curved RC beams.
- To propose conclusions on the effectiveness of different applications of CFRP shear retrofitting to its capacity, failure mode, cracking and deflection of the out of plane curved RC beams.

1.3. Methodology

i). Conduct literature review to investigate on FRP material specifications, use of curved beam retrofitting and modes of failure.

ii). Conduct literature review on application of CFRP retrofitting in RC beams in consideration of and recognize on research gaps areas for curved beam.

iii). Conduct theoretical capacity calculation for bending and shear.

iv). Cast RC beams are cast in two series to differentiate over flexural and shear.

v). Conduct experimental program to application of CFRP plate for out-of-plane curved concrete beam for strengthening flexure. Fibre application done in two different ways to analyse for end anchorage effect.

vi). Prepare curved control beam specimens respect to above beam specimen prepared to compare the enhancement.

vii). Conduct experimental program to application of CFRP fabric for out-of-plane curved concrete beam for strengthening shear. Fibre application done in two different ways to analyse effect of the zone of application.

viii). Prepare curved control beam specimens respect to above beam specimen prepared to compare the enhancement.

ix). Load beam specimens by four-point bending method until failure with monitored deflection at mid span.

x). Plot Load vs. Defection curves against each beam specimen.

xi). Analyse and compare effectiveness of CFRP usage using results of experimental data obtained by the observation and record of crack initiation/propagation, FRP/ RC failure and load capacity with deflection.

xii). Compare results of theoretically predicted with the experimented actual.

xiii). Derive conclusions using the findings of the analysis and recommendations for any future improvements.

1.4. Scope of the Research

Experimental investigation of horizontally curved beams of same radius of curvature, loaded under four point out of plane loading and enhancement using CFRP for flexural and shear capacities with an improvement for each. In addition, comparison of theoretical load carrying capacities over actual load carrying capacities, failure modes, initial cracking and analysis of load vs. deflection behaviour.

1.5. Significance of Research

Curved structural elements are ample in new age development. For secondary concrete strengthening applications, FRP gained popularity over conventional structural strengthening techniques like fixing of supplemental steel frames and other elements. Therefore, this research can contribute to fill the gap of lack in horizontally curved, out of plane loaded beam strengthening experiments using CFRP and research on their degree of enhancement of shear and flexural capacity.

1.6. Outline of research thesis

Chapter 1: Introduction

A general introduction is given in this chapter including the purpose of the research and methodology.

Chapter 2: Literature review

A detailed study of past researches in the subject area and summarization is presented in this chapter. The purpose of this chapter is to recognize the research gaps existing in the relevant research areas and identifying areas to be developed.

Chapter 3: Experimental program

This chapter explains the test specimens, material properties, testing and instrumentation, experimental results and result discussion.

Chapter 4: Theoretical Analysis

This chapter presents calculation using standard codes and guides to predict capacities, failure loads, modes and comparison with experimental results.

Chapter 5: Conclusion

This chapter culminates the outcomes of the research along with recommendations for future research studies.

CHAPTER 2: LITERATURE REVIEW

2.1 Applications and use of FRP

FRP systems are useful to rehabilitate or structurally restore the strength of deteriorated concrete structural members and to enhance the capacity of a sound structural members to resist its increased loads (Nur Yazdani et al., 2016). These alterations can be due to changes in use of the structure with time or initial design or construction errors. The selection of the type of FRP system and strengthening technique should be determined by a licensed design professional. Carbon Fibre Reinforced Polymers (CFRP) are used for manufacturing in many industries like automotive applications, marine, aerospace parts, sport goods like golf clubs, skis, tennis racquets, fishing rods and bicycle frames (Hayes, 1985).

Suitability of an FRP system for a particular application need to be assessed by performing determination of concrete substrate condition, deficiency and causes identification and existing load-carrying capacity. The documentation of maintenance history, specifications, design drawings, as-built documents should be reviewed and overall evaluation included by a comprehensive field inspection. In addition, documents on structural analysis and field test reports are vital. (Alkhrdaji, 2015).

The existing conditions of the member like reason for cracking or spalling, reinforcement provided and cover of steel, concrete compressive strength in-place, existing concrete soundness and dimensions should be determined by a field inspection. It is important to consider active corrosion presence and degree, location of corrosion presence if any, covering all areas of FRP system bonded to existing structure (ACI 440.2R-08).

With the use of the gathered information of the field investigation, load-carrying capacity of the existing structure can be reviewed, using analytical methods of review of drawings and design calculations. As appropriate for application, overall evaluation process can be incorporated with load tests or other methods (ACI 437R-19).

2.2 Material Properties

2.2.1 Types of fibres

In the construction industry mainly three types of fibres are used for FRPs which are carbon, glass and aramid. Basalt fibres have been gaining attention last few years as an alternative for glass fibres nevertheless, it is not common as the other three types of fibre. The selection of fibres should be done considering various factors: cost, specific strength requirements and specific environmental conditions (Karaca and Buyukozturk, 2002; Nanni et al., 2014). Material properties of different types of fibre are given in Table 1.

Table 1: Material properties of different fibre types (Giuseppe Simonelli, 2005)

Fibre	Tensile strength (N/mm^2)	Modulus of elasticity (kN/mm^2)	Elongation (%)	Specific density
Carbon: high strength	4300-4900	230-240	1.9-2.1	1.8
Carbon: high module	2740-5490	294-329	0.7-1.9	1.78-1.81
Carbon: ultra high module	2600-4020	540-640	0.4-0.8	1.91-2.12
Aramid	3200-3600	124-130	2.4	1.44
Glass	2400-3500	70-85	3.5-4.7	2.6

Carbon fibre - Carbon fibres are classified into two separate types based on Young's modulus as high modulus Carbon fibres and low modulus carbon fibres due to wide variation of strength and stiffness of the material which depends on the manufacturing process. PAN-based carbon fibre mostly used for Civil Engineering applications due to its high strength and relatively higher Young's modulus. Even though pitch-based carbon fibre has higher Young's modulus, their strength is relatively lower, hence it is used in aerospace applications (Pooja Bhatt and Alka Goe, 2017).

Glass fibre - Mainly three types can be recognised as most commonly used in civil engineering applications: Electrical glass fibres (E-glass), High Strength glass fibres (S-glass) and Alkali Resistance glass fibre (AR-glass). E-glass provides superior corrosion resistance and electrical insulation while S-glass provides higher strength and stiffness. However, S-glass is costlier compared to E-glass. AR-glass provides much more superior alkali attacks whereas E-glass and S-glass are weak against alkaline induced corrosion compared to other alternative types of fibre (Nanni et al., 2014).

Aramid fibre - Aramid fibres are organic synthetic material with superior mechanical properties: high strength, high toughness, high impact resistance and high resistance for creep and rupture. Due to its high strength and low density (low weight), aramid fibres are used in the sports industry and military applications.

Basalt fibre - Basalt fibres are relatively new to the civil engineering industry and research studies are ongoing to improve the properties of the material. It is mainly used as an alternative to glass fibres due to its relatively superior strength, stiffness and low manufacturing cost due to ease of production and high availability of Basalt material (Nanni et al., 2014).

In comparison of above, in terms of strength, composites are better. However, on weight basis, cost of composite materials are higher than for steel by several times. Typical stress - strain curves for unidirectional composites subjected to a monotonic loading are shown in the Figure 2.

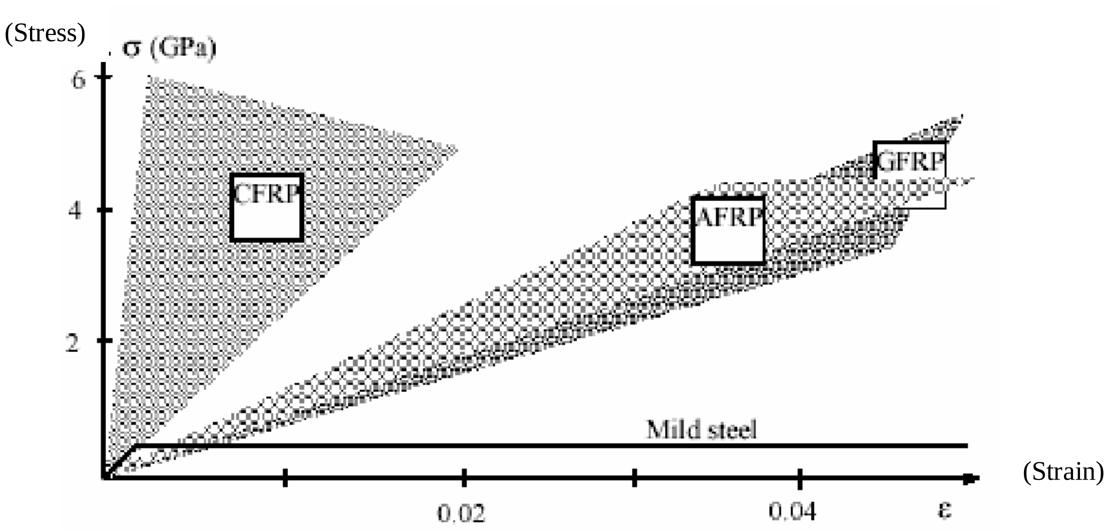

Figure 2: Uniaxial Tension stress - strain diagrams for unidirectional FRPs of Carbon, aramid, glass and steel materials (FIB Bulletin 14, 2001)

In selection of FRP composites for strengthening purpose, long-term durability and constructability are also vital in selecting based on mechanical performance. Therefore, without treating FRP to be used as a blind replacement of steel, necessary consideration should be given to all the design issues (Setunge et al., 2002).

2.2.2 Carbon fibre reinforced polymer (CFRP)

Carbon Fibre Reinforced Polymer (CFRP) is defined as a Polymer Matrix Composite material. Reinforcement is provided by carbon fibres. In form of either continuous or discontinuous carbon fibres of diameter approximately 10 µm which are commonly woven into a cloth, the reinforcing dispersed phase exist. Although Carbon fibres are very expensive compared to other material, comparatively they possess the highest mechanical properties for modulus of elasticity and strength per weight (SubsTech, 2012). The main disadvantage of carbon (Graphite) fibres is catastrophic mode of failure, the brittle nature.

Due to the following properties, Carbon fibres have become widespread in usage as a reinforcing polymer matrix.

- Very high modulus of elasticity which at all times exceeding that of steel;
- Low Density : 1800 kg/m³;
- High tensile strength can be in the level of 7 GPa;
- High chemical inertness.

The types of carbon fibres that are generally in use are as follows:

- Ultra high modulus (UHM) in which Modulus of elasticity > 450 GPa
- High modulus (HM) in which Modulus of elasticity is in the range 350-450 GPa.
- Intermediate modulus (IM) in which Modulus of elasticity is in the range 200-350GPa.
- High tensile, low modulus (HT) in which Tensile strength > 3 GPa and Modulus of elasticity < 100 GPa.
- Super high tensile (SHT) in which Tensile strength > 4.5GPa.

Classification of Carbon fibres can also be done according to its method of manufacture. The most popular type is the PAN-based carbon fibres which are produced by stretching filaments from polyacrylonitrile precursor by conversion of polyacrylonitrile (PAN) precursor and process of thermal oxidation. The filaments are at first held in tension. Then for several hours subjected to Carbonization in a Nitrogen atmosphere. Non-carbon elements like O, N and H volatilize resulting in fibres enrichment with carbon during this stage. Finally, the fibres are subjected to Graphitization at about 2500°C temperature (SubsTech, 2012).

Carbon fibres which are manufactured from pitch are classified as Pitch-based carbon fibres. In the process, spun filaments of coal tar or petroleum asphalt are taken and cured at temperature of 315°C. Then subjected to Carbonization in a Nitrogen atmosphere. In the manufacturing procedure of CFRP, the most prevalent matrix materials are the thermosets like epoxy, polyester and thermoplastics like polyamide. Pultrusion method, open mold processes and closed mold processes are the basic methods of manufacturing of CFRP. CFRP materials has the ability of provision of reinforcement in two perpendicular directions, due to the presence of the laminate structure. (SubsTech, 2012).

Characterization of CFRP can be done based on its properties by either light weight or very high modulus of elasticity-to-weight ratio or high strength-to-weight ratio or good corrosion resistance or high fatigue strength or very low thermal expansion coefficient or high electric conductivity or low impact resistance or high cost (Babu and Bhattacharya, 2020).

2.2.3 Available forms

2.2.3.1 Fabric form

Basically two forms available;

• Sheet material form, either fibres on a removable backing sheet (unidirectional in general, however available in bi-axial and tri-axial arrangements) or woven rovings.

• Fibres that are manufactured pre-impregnated with resin (“prepeg” material), which can be cured after in place by heat or other means.

The right fabric for the job is determined by the application. The amount and type of fibre used determine the qualities of the sheet materials. Another factor to consider is the way the fibres are laid out; a parallel lay fabric has unidirectional qualities, but two-dimensional properties possessed by woven fabric. Approximately 70% of the fibres in woven fabrics are located in the “strong” direction, whereas 30% are in the transverse direction. The observation was given in the research that the woven material's strength is greatly reduced by the kinking of the strands. The material's thickness can be as thin as 0.1 mm (when the fibres are attached to a detachable backing sheet) as observed and it comes in widths of dimension 500 mm or more (Giuseppe Simonelli, 2005).

2.2.3.2 Plates

Pultrusion is commonly used to create unidirectional plates. Fibres are pulled off in a precisely controlled manner as continuous rovings through a medium of resin bath that impregnates the fibre bundle. The bundle then pushed through a form of die, which compacts the fibre-resin mixture and shapes it into the desired shape. This die is heated which make the resin to set and cure. It allows the completed composite sets to be drawn off using a reciprocating clamps or by means of a tension device. This process enables about 65% of fibres to be integrated in the cross section resulting, relatively high stiffness and strength attained in the longitudinal direction. Since in most of the fibres, the transverse direction strength will be very much lower compared to longitudinal.

Pultruded plates are supplied in widths in the range of 50 and 100 mm and thickness around 1-2 mm. Since pultrusion is a continuous process, fibre material can be fabricated in very long lengths. In the coil form with a diameter close to 1 m, thinner material is provided. These plates can be easily cut into desired length at site using a common guillotine. In production of components in automotive and aerospace industries, the prepeg process is widely used. The plates can be produced in up to 12 m length and thickness may be varied upon the intended application. Further, it is produced in 1.25m width and up to 30 mm thickness as well. Plates typically have a fibre volume fraction of 55%. To improve the handling strength, can incorporate 10% fibres. (Giuseppe Simonelli, 2005).

2.2.3.3 Rods

Manufacturing of fibre rods is done through pultrusion process which is a similar to extrusion of thermoplastic and Aluminium. In this process, carbon fibres pulled and epoxy resin mixed through heated forming dies. Fibre rods of uniform cross section and continuous stretches of rods can be formed by this process, which take on shape of the die. Saturation with epoxy resin is done while they are pulled through the die followed by heating for the resin-hardening or polymerization process.

The rods of low weight, rigid, low thermal expansion coefficient and straight are produced in the extrusion process in which outer diameter tolerance is controlled very well. Since fibres run along the rod length on the same axis, excellent linear strength is ascertained. In bending applications and axial tension or compression uses carbon fibre rods performance is satisfactorily well. Experimental and analytical comparison to study on the flexural behaviour of concrete beams which were all reinforced by sandblasted carbon fibre based composite rods was carried out in previous research. 3 nos. control beams with steel reinforcement and 12 beams were tested to find strength, failure modes and deformation. Comparison made in the analysis generating theoretical strength and their moment curvature relationship. Pull out test results revealed that sandblasted rods bonding isn’t a main concern in this. Though, limiting factor in the design was identified as the excessive deformation in attaining the anticipated moment capacity of the tested beams (Thiagarajan and Ganesh, 2003).

2.2.4 Types of Matrix resins

The main purposes of the matrix are to transfer stresses to fibres as mentioned above. Additionally, it provides protection for fibres and shear & compressive strength of the composite. Two types of matrix materials can be recognized, namely, thermosetting polymers and thermoplastic polymers. Former is usually used in civil engineering applications. Thermoplastic and thermoset polymers usually are liquid or semi-solid and once they are cured it will result in a solid, comparatively strong rigid material. However, thermoplastic polymers can be transformed back to original liquid form even after the curing process which makes them highly unsuitable for civil engineering applications whereas, thermoset materials retain their strength and rigidity once curing is done which is highly suitable for FRP polymers in civil engineering applications. There are three main types of thermoset polymers that are currently in practice, which are epoxies, polyesters and vinyl ester resins. Furthermore, fillers are usually used to engineer the properties of polymers and reduce the overall cost of the materials (Grumezescu and Grumezescu, 2019; Karaca and Buyukozturk, 2002; Nanni et al., 2014).

Epoxies **-** Epoxies are dominantly used in civil engineering applications for the reason of their superior mechanical and physical properties and low shrinkage compared to alternatives. Even though, there are disadvantages to epoxies: the cost of epoxies are higher, long curing time and difficulty of application to concrete, it is preferred over other alternative materials due to the aforementioned advantages. Furthermore, Good adhesion to fibres, superior performance against environmental conditions and high compatibility with all four main types of fibres can be recognized as other important properties of epoxies (Nanni et al., 2014).

Vinyl Esters **-** Vinyl esters typically show close superior mechanical properties of epoxies, however, has a higher cost compared to epoxies. Vinyl esters encouraged to use in GFRP over epoxies even though it has a higher cost, due to its highly impressive resistance for alkaline environmental conditions and good wetting and adhesion with glass fibres (Nanni et al., 2014)..

Polyesters **-** Polyesters show the optimum cost to strength characteristics. Two types of polyesters are commonly used: orthophthalic and isophthalic acidic polyesters. Iso polyesters have superior mechanical properties and superior thermal and chemical resistance compared to ortho polyesters, however, costlier. Even though there are advantages for polyesters as mentioned before, it is usually discouraged to use in FRPs due to low strength and low resistivity to environmental conditions compared to epoxies and vinyl esters (Nanni et al., 2014).

2.3 Strengthening limits of FRP

The limits are imposed for strength of a FRP system for the purpose of prevention against failure if subjected to damage to the FRP. Therefore, limitation is exerted on the member load carrying capacity in retrofitted structure. FRP reinforcement loss should not result in failure of member ultimately under service load.

The design considerations of a FRP system intended to increase the strength of a member should include a broad identification of load limitations, load paths, temperature effects and environment, loading concerns and steel corrosion effects on integrity of FRP system (ACI 440.2R-17).

2.4 Effect of temperature

At high temperatures most FRP materials tend to degrade its characteristics. Externally bonded FRP systems strength is presumed that be completely loss under fire condition. If the critical temperature of the FRP is not exceeded the degradation effect can be minimised up to certain extent otherwise. Provided that the member itself solely can withstand all service loads effectively during a condition of fire. Therefore, coatings, resins, insulations or other means are generally used to enhance the fire resistivity of the retrofitted RC member (Burke et al., 2013).

Design of FRP installed members should be done according to all applicable building and as well as fire codes. According to building classification type, flame, smoke generation ratings should be satisfied.

2.5 Bonding effect with concrete substrate

For bond-critical applications, concrete substrate strength is an essential parameter. Repairing of substrate is essential where deteriorated concrete surfaces present and sound surface of concrete should be formed. The degree of corrosion, distress of concrete and damages should be accounted prior to prior to the FRP application. Alkali-silica reactions, laminar cracking or other types of concrete deterioration should be considered under the substrate repairing (Alkhrdaji, 2015).

The design stress development strength by bond is require to be integral of concrete substrate. In order to transfer forces to the FRP system, the substrate should possess adequate direct tensile and shear strength. Design stresses development in the FRP in contact-critical applications occur through concrete section deformation or dilation.

FRP will not prevent ongoing corrosion of reinforcement. Without repair of corrosion effects, placing FRP on concrete substrate is not recommended (ACI 440.2R-17).

2.6 Shear strengthening

Experimental studies suggest that the application of FRP external reinforcement increases the shear resistance of RC beams. The application of FRP can be done in three ways: fully wrapping, U-socketing and side bonding as shown in Figure 3.

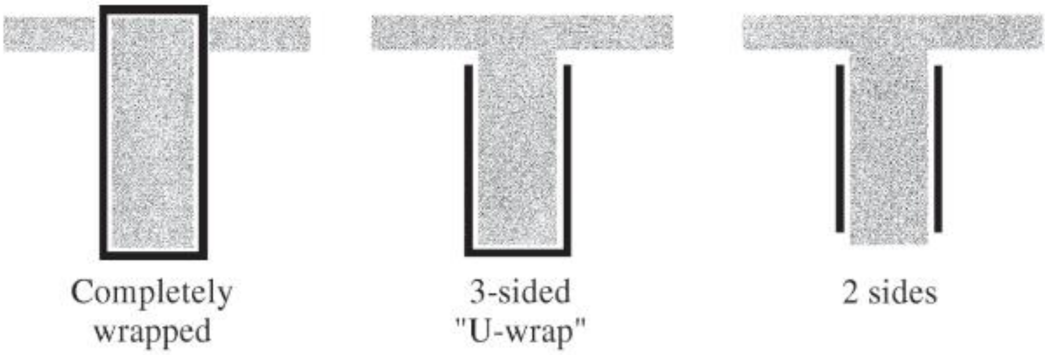

Figure 3 : Different FRP application methods for the shear enhancement (ACI Committee 440, 2017)

Shear strengthening of straight concrete beams experimented in laboratory with placement perpendicular to the shear crack. Concrete compressive strength will decide on the shear strengthening limitation to have more strengthened structure. Strain measurements in such showed that with the reduced thickness of the fibre material, the effective utilisation of fabric be manured. The theoretical and actual results have quite good agreement in research experiment of two beams with strain gauges (Bjorn Taljsten, 2003). As per the observations for design, approximately 0.55 of the maximum measured strain was recommended. In the design only failure at anchorage was not present, hence suggested field application with anchorage for CFRP strengthening.

In some studies, the experimental investigations carried out for externally bonded FRP to beam soffit to analyse for shear strengthening. Changing of stirrup spacing in shear zone, varing reinforcement beam series were casted. Beam series were grouped based on the flexural reinforcement ratios and extent of layers of CFRP strengthening. Specimens were tested by four-point loading test in which a shear span to depth ratio is around 3. Shear failure of all specimens observed and until failure the load vs. midspan deflection curves were plotted. Predicted shear strength from design codes and models (i.e. ACI318-11 simplified; CSA-2004) compared with the results of experimental data based on the cracked neutral axis depth (Hawileh et al., 2015).

As per the findings of research, over the control beams, 10 to 70% increase of shear strength is gained over the control specimens. Further, the increment of CFRP no of layers has proportionally enhanced shear strength. Another observation is that the specimen with lesser steel reinforcement has shown higher shear strengthening percentage than the higher reinforced. However, as the number of CFRP layers increases, a decrease in the percentage of escalation of shear strength was observed. Steeper diagonal shear cracks observed when the amount of longitudinal reinforcement ratio increased. In addition, post cracking stiffness increment also observed (Hawileh et al., 2015).

In previous research experiments, shear behaviour of CFRP retrofitted beams that are weak under shear were tested in simply supported loading condition was studied. The varied parameters were shear reinforcement, amount of CFRP, CFRP placement and shear span to effective depth ratio. As per the results, significant shear capacity enhancement observed due to CFRP addition and the parameters tested have varied its efficiency. Increase in the shear strength of 40–138% was achieved in a previous study (Ahmed Khalifa and Antonio Nanni, 2002).

As per the test results (Ahmed Khalifa and Antonio Nanni, 2002), for beams without shear reinforcement, contribution of CFRP benefits the shear capacity is at a greater degree than for beams with adequate shear reinforcement.

The study summarized influenced of the span to effective depth ratio for contribution of external CFRP reinforcement to the shear capacity. Increasing the amount of CFRP not result in a proportional increment in the shear strength and recommendation was provided to use end anchoring to prevent FRP debonding.

Suggestions and recommendations for future research were provided to identify the link of shear contribution of FRP with steel reinforcement ratio and strength of concrete as parameters. The strengthening effectiveness of FRP has to be addressed in the cases of short and very short shear spans in which arch action governs failure, interaction between the contribution of external FRP and internal steel shear reinforcement, shear design algorithms to be expanded to investigate use of the glass fibre or aramid fibre for the strengthening to compare (Ahmed Khalifa and Antonio Nanni, 2002).

Studies were performed for straight RC beams wrapped with CFRP and differentiated by provision of end anchorages. It shown that increment in stiffness, capacity and ductility can be gained in all CFRP wrapped RC beams. Initial cracking load is also higher than of control beams as observed in wrapped beams and fine crack distribution was seen throughout the span (Asad ur Rehman Khan and Shamsoon Fareed, 2014).

CFRP wrapped specimens showed maximum 16.7% increase of ultimate load carrying capacities (than control beams), whereas it increased up to a maximum of 20.8%. Strengthened beams tested at smaller span to effective depth ratio were found to fail in shear, though adequate shear reinforcement provided. Failure modes differed in strengthened beams with smaller span to effective depth ratio which may be due to the effect of end anchorages. As expected flexure failure observed in beams tested at higher span to effective ratio (Asad ur Rehman Khan and Shamsoon Fareed, 2014).

In previous research effective increase in initial cracking loads, stiffness, improved crack patterns and ductility observed in beams retrofitted using CFRP. The effect of distance from support to fibre end is investigated with use of single layer of fibre to investigate on debonding failure. With the use of two layer of fibres for strengthening, after a certain length of second layer of fibre, beam performance becomes constant. Under this condition, performance of CFRP installation is less cost effective (L.J. Li et al., 2006).

Non cracked retrofitted and pre cracked repaired RC beams U-jacket FRP continuous beams were experimented to evaluate the size effect (Long Nguyen-Minh and Marian Rovnak, 2015). It recognised for above two cases degree of strengthening was different. Increase in shear capacities of retrofitted beams was inversely proportional to the beam sizes. In repaired beams, due to pre-cracking, beam size effect was disregarded. Therefore, effect of beam sizes were different for repaired and retrofitted beams.

The effect of beam sizes did not influence on maximum values of strain. Increase of jacket strains in retrofitted beams observed to decrease over beam size increment. The distribution of strain observed at a high gradient in the longitudinal direction. Non strengthened beams showed higher rebar strain gradients than repaired beams. Repaired beams showed higher jacket strain than retrofitted beams. Yielding of Shear and flexural reinforcement did not encounter in retrofitted beams. The frame-tie action act predominantly prior to shear failure of beams. (Long Nguyen-Minh and Marian Rovnak, 2015).

2.7 Flexure strengthening

Experimental studies suggest that the application of FRP external reinforcement increases the flexure resistance of RC beams. The application of FRP can be done in Near Surface Mounted (NSM) or lamination methods as shown in Figure 4.

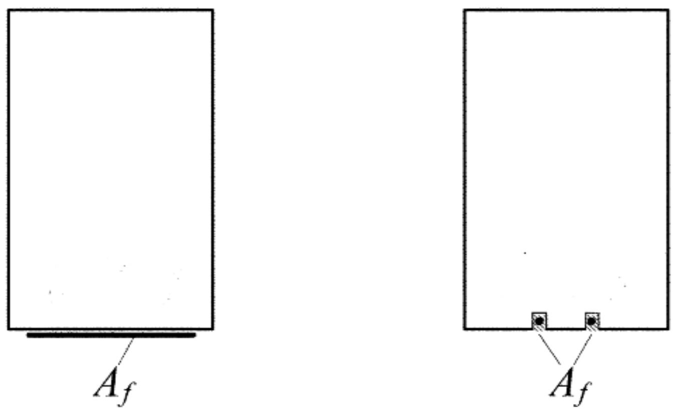

Figure 4 : Different FRP application methods for the flexure enhancement (ACI Committee 440, 2017)

Behaviour of straight beams has been studied under several researches with provided CFRP, targeted to flexural enhancement. For flexural strengthening of RC beams, total ten beams were cast and tested over an effective span of 3000 mm up to failure under monotonic and cyclic loads (R. Balamuralikrishnan and C. Antony Jeyasehar, 2009). Eight concrete beams designed under reinforced were strengthened with CFRP fabric. Bonded CFRP laid at beam bottom in single layer and two layers parallel to beam axis and tested. Two beams were tested as control beams. Responses of beam was evaluated for stiffness, strength, energy absorption and failure modes.

ANSYS software was used to predict the load vs deflection relationship and moment – curvature theoretically. Results of experimental testing compared with the numerical software analysis outputs and conclusions made are presented as follows (R. Balamuralikrishnan and C. Antony Jeyasehar, 2009).

Externally bonded CFRP can influence substantial increase flexural strength, where, it is in the range 18-20 % in single FRP layer and 40-45 % in two FRP layers, cyclic loading of static and compression.

Reduction of deflections was observed in each loading stage, where, it can conclude that enhancement of stiffness of strengthened beams has occurred.

Strengthened beams shown 80% decrease of deflection at ultimate load than control beams. CFRP strengthened all beams tested were failed by flexure n both single layer and two layers. Premature brittle failure was not observed in any (R. Balamuralikrishnan and C. Antony Jeyasehar, 2009).

The investigation also revealed that epoxy system can ensure proper bonding in CFRP in single or two layer applications and considerable ductility enhancement in whole structure.

Experimental results exhibit flexural strength enhancement close to 20% and 45% in two beam types relative to control beams. The theoretical analysis results are close to the experimental results and minimum of 2 layers of CFRP required to have the acceptable results. (R. Balamuralikrishnan and C. Antony Jeyasehar, 2009).

2.8 Behaviour of CFRP Strengthened straight beams

Failure modes due to debonding can be generally observed in various types. As demonstrated in Fig.5, (a) CFRP central rupture, (b) cover separation in concrete, two types of interfacial crack debonding shown in (c) and (d), (e) debonding that occur intermediately, (f) interlaminar FRP shearing, (g) fibre slippage within matrix, (h) crushing of concrete and (i) failure by shear (Hui LiLye et al., 2020).

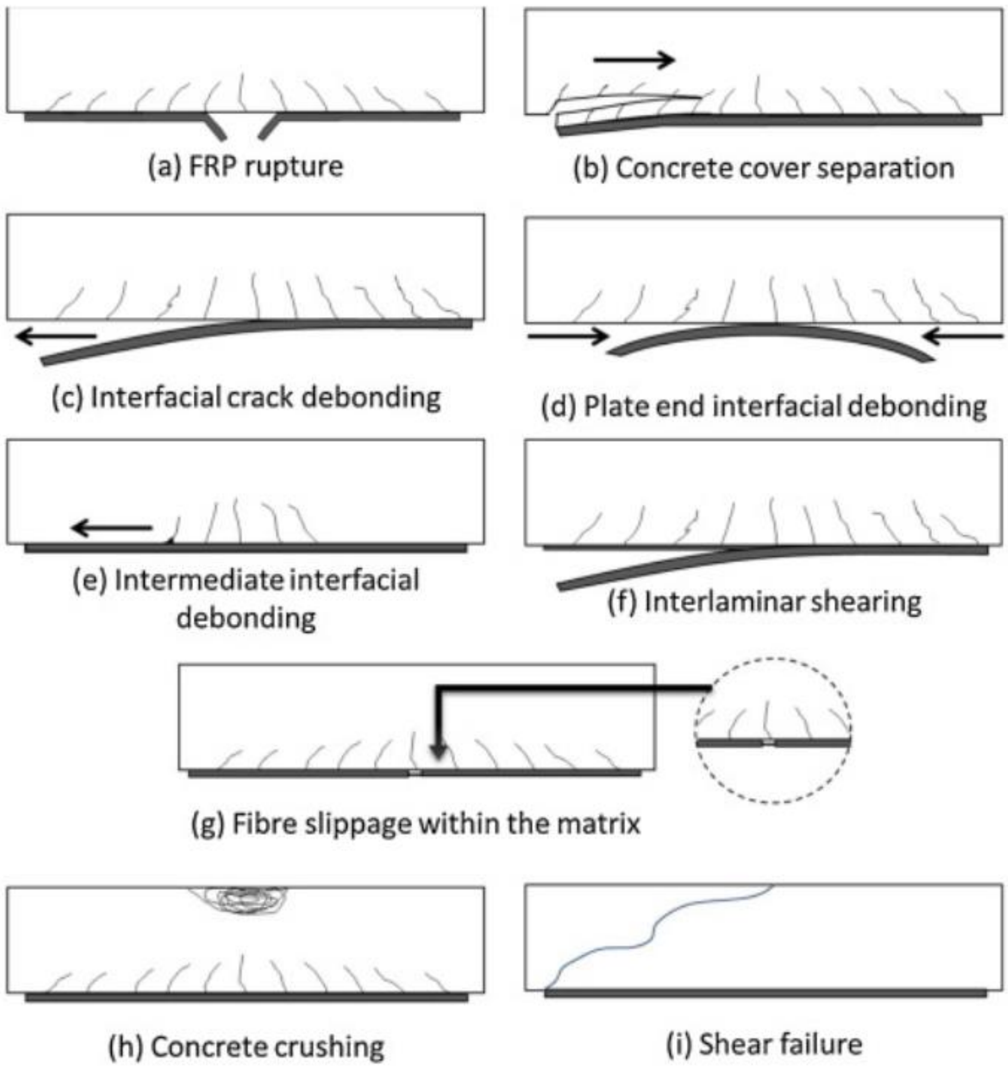

Figure 5: Debonding & other failure types of CFRP strengthened beams

Stresses that concentrate interracially and locally at the CFRP cut-off point, as well as flexural and shear cracks in the structure, induce these failures. Efficient stress transfer from CFRP to the concrete structure takes place in mode (a) failure, and then the strain capacity of CFRP is fully utilized until the rupturing of structural member. Shear stress tend to propagate from one end to other along the full stretch of the structure, causing modes (b) and (c). In particular, the shear fracture formation close to CFRP in mode (b) is typically severe, and it is exacerbated by stress that causes the concrete cover to pull away from the rebar. In mode (c) delamination of CFRP occur from the concrete member (Hui LiLye et al., 2020).

Furthermore, mode (d) debonding CFRP detach and it propagate inwardly to middle of the beam, which is called end debonding. In mode (e) interfacial debonding occur intermediately due to propagation of fracture and results in debonding. Likewise, in mode (f) interlaminar shearing demonstrates that the concrete and CFRP bonding much stronger than bond of shear, which usually happens when CFRP portion fails and leaving theremnant portion. Mode in (g) is caused by a lack of bonding between the fibre and matrix interface, particularly at the fibre-matrix interface. The dominant tensile reinforcement ratio will result in crushing of concrete as seen in mode (h), which will prevent CFRP debonding. Finally, excessive flexural strengthening will result in shear failure, mode (i) Indeed, premature debonding has hampered both concrete and CFRP's maximal capacity (Hui LiLye et al., 2020).

In view of similar research study, the historical Horsetail Creek RC Bridge which was a bridge with beams deficient in shear and moment capacity (Damian I. Kachlakev- Oregon State University, 2000). Therefore bridge was required to be retrofitted to enhance load-carrying capacity without damaging its aesthetic appearance.

FRP retrofitted beams were tested subsequently to validate the load capacity enhancement, since FRP is an innovative technique where the increase in RC beam capacity gained successfully. The study also included investigation of strain and deflection relationship over loading in RC retrofitted beams of bridge. Similar beams to actual full-size bridge beams were tested in the laboratory to accomplish the adequacy for actual traffic loads.

As per the conclusions, the strengthened beams of Horsetail Creek Bridge 50% more static load shear capacity, 99% more static load moment capacity 30% stiffer than the non-strengthened beams. The strengthened Horsetail Creek Bridge crossbeams are the unstrengthened beams. Diagonal failure by tension occured in beams retrofitted with FRP only for flexure. To resist diagonal cracking CFRP wrapped in sides sufficiently. Beam strain is reduced as seen in the experiment due to reduction of deformation which should not be solely relied in the design (Damian I. Kachlakev- Oregon State University, 2000).

Flexure failure in midspan occurred in bridge beams only retrofitted for shear by GFRP. Tension reinforcement yielding occur prior to concrete crushing. The absence of stirrups is mitigated by shear retrofitting and failure is generally caused by yielding steel. Ultimate deflections of strengthened beam are two times of the control beam which failed by tension cracking. 23 percent increase in initial cracking load was observed as a result of stiffness enhancement by flexural CFRP which also cause reduction in strains and stresses at a cross section under subjected load (Damian I. Kachlakev- Oregon State University, 2000).

2.9 Behaviour of pre-cracked straight beams strengthened with CFRP

Research study on pre-cracked continuous straight beams were carried out to evaluate CFRP retrofitting effects (Noorwirdawati Ali et al., 2012). CFRP strips wrapped straight RC beam specimens prepared, changing wrapping schemes and orientation of CFRP strips and a control beam. while the other four beams were pre-cracked prior to wrap with CFRP strips. The conclusions made on ultimate load, failure modes and crack patterns are as follows.

The failure modes of 4 sides wrapped beams was shear and CFRP rupture. In 3 sides wrapped beams additionally CFRP debonding from member surface observed.

Compared to the beam specimens with CFRP orientation of 0º/90º, lesser cracks observed in the beams specimens with CFRP strips oriented 45º/135º direction. Therefore, in beam crack propagation control, CFRP placement orientation 45º/135º is very effective as per the experimental results. (Noorwirdawati Ali et al., 2012).

Compared to control beam specimens, shear carrying capacity observed greater in retrofitted beam specimens. Higher deflection could be preventing by placing CFRP sheet throughout the bottom of the beam. Although deflection was lower than the permissible value, overall deflection can be reduced by placement of CFRP along entire beam bottom.

Compared to the beam specimens with CFRP orientation of 0º/90º direction, higher stiffness observed in the beams specimens with CFRP strips oriented 45º/135º. In resisting shear, CFRP elongation supports considerably by restraining against crack widening and excess strain at the concrete surface (Noorwirdawati Ali et al., 2012).

Further as per experimental study to investigate the behaviour of structurally damaged full-scale reinforced concrete beams retrofitted with CFRP laminates in shear or in flexure (Yasmeen Taleb Obaidat et al., 2011) with varied reinforcement, CFRP length and CFRP placement. As per the conclusion made, the retrofitting showed efficient enhancement of flexure and shear than control beams and its dependable on length of CFRP. The failure mode observed was mainly plate debonding and stiffness and strength restoration of beams was also satisfactory.

2.10 Debonding failure

In applications of strengthened RC beams by means of externally bonded FRP, the types of debonding failures mostly encountered are the Plate end debonding or interfacial debonding.

(S. T. Smith and J. G. Teng, 2002). In the experiment, beam specimens strengthened with FRP plates in one series and the other series with steel plates. All beams classified in following three categories as models for shear capacity, concrete tooth and interfacial stress. The relationship between each of these models were analysed on a theoretical basis. Experimental database accumulated through previous literature of RC beams which failed by plate end debonding and used to assess the performance of specimens.

Prior to reach ultimate load failure of concrete beams debonding was observed, the greatest strength range of CFRP was unable to witness. It concludes that failure by debonding has significant influence over initial cracking load, rather than on ultimate load, stiffness and ductility. The effect on crack patterns is trivial due to debonding as per the findings (L.J. Li et al., 2006).

2.11 Curved beam applications

Curved beams are used in curved floors in buildings, balconies, curved ramps and halls, circular reservoirs and similar structures. Due to the attractive appearance, curved buildings are particularly popular among architects and Engineers. Curved structural elements, such as curved beams or curved walls, make up this structure. Curved beams are beams that are curved before a bending moment or a load is applied. Vertically curved beams and horizontally curved beams are the two most common types of curved beams. Curved beams with changing curvature, slanted from the horizontal plane and a combination of vertical and horizontal curvatures are examples of these types of beams. Unit strains in curved beams are not proportional to the distance from the neutral surface and the centroidal axis does not coincide with the neutral axis dissimilar to the condition in straight beams.

Figure 6: Vertically and horizontally curved RC applications

2.11.1 Vertically curved in-plane loaded beams

Vertically curved beams, such as curved members in arches and bents, are described as beams that are curved in space and loaded in-plane (Figure 7). Curved girder members in circular constructions and domes, curved beams in curved parts of bridges, and curved elevated highway ramps are examples of horizontally curved beams.

Due to their shape, the loads nearly entirely transfer axially, causing nominal stresses on cross-sections and minor bending moments, vertically curved beams have substantially superior structural integrity than straight beams. Hence, the ultimate capacity of vertically curved beams depends on the ultimate compressive strength of the concrete rather than the ultimate tensile capacity of concrete and since the compressive capacity of concrete is much greater compared to the tensile capacity, vertically curved beams have much higher structural integrity compared to horizontally curved and straight beams (ProQuest 2017).

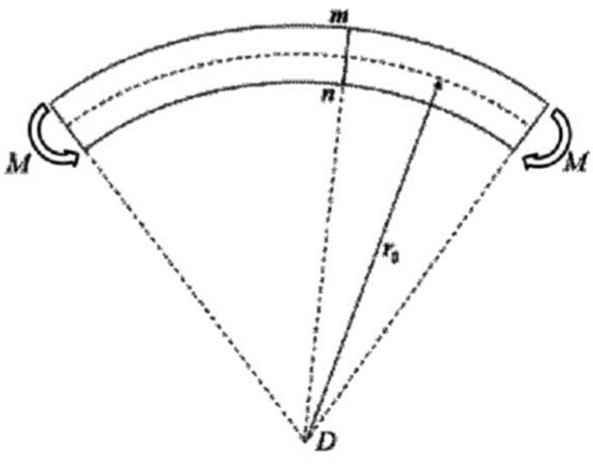

Figure 7: Vertically curved in-plane loaded beam

2.11.2 Horizontally curved, out-of-plane loaded beams

When an out-of-plane load is applied (Figure 8) to a horizontally curved beam, torsional stresses, as well as flexural and shear stresses, are created. A straight beam, on the other hand, will only have flexural and shear stresses. However, in a straight beam, there will be only flexural and shear stresses. This additional torsional stress in curved beams will cause to reduce the beams' shear capacity by adding a component from torsional stresses to shear stresses subsequently causing the beam to fail in shear at a lower load. Hence, horizontally curved beams are more critical and vulnerable to shear failure compared to straight and vertically curved beams.

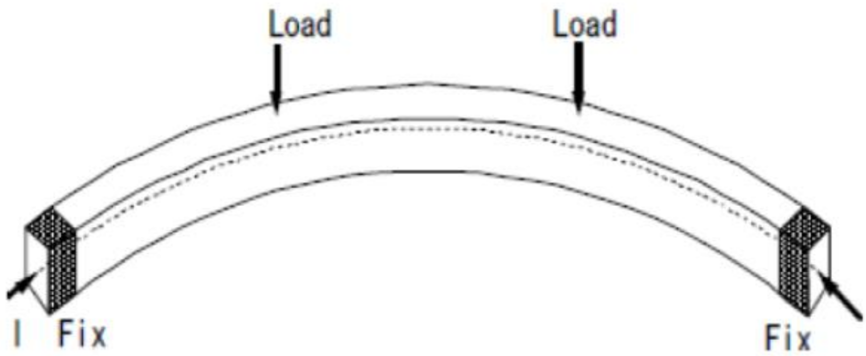

Figure 8: Horizontally curved, out-of-plane loaded beam

Through experimental studies, RC curved beams were tested find the influence of axial force and the shear span depth ratio towards fracture properties (T. Tamura & H. Murata, 2010). Based on the test results, the following conclusions were made.

With the change of shear span to depth ratio, strength change rate of curved beams closes to straight beam. The rate of change of the ultimate strength of the curved beam is close to that of the straight beam. In curved beams with smaller curvature, the ultimate strength becomes large when axial compression was applied. However, in this experimental study, for the case if large curvature beams, the ultimate strength became small when axial compression was applied. (T. Tamura & H. Murata, 2010).

2.12 Inplane loaded curved beams retrofitting

In view of research on this scope, an experimental program was conducted to understand the behaviour of flexurally-reinforced RC beams with concavely-curved soffits strengthened with

CFRP (K. Al-Ghrery et al., 2019). Five RC beams were constructed and tested up to failure. 3 nos. beams were curved soffit RC beams; one was un-strengthened and two identical beams were strengthened with CFRP fabric. The other two were beams of flat soffit, one beam was unstrengthened and one was strengthened using CFRP fabric. All beams were 2700 mm long, 140 wide and 260 mm deep at mid-span. The depth of the curved-soffit beams near the support ends was 340 mm. The curved soffit beams were constructed with a degree of curvature of 20 mm per metre with a chord length of 2000 mm. The experimental program results are used to compare the FE modelling analysis results.

The results show that curvature of 20 mm per metre can cause efficiency reduction of FRP strengthening by 17.8%, and beams experience premature CFRP de-bonding generated due to the high concentration of stresses generated by the induced curvature. Interfacial cracks are the foremost failure mode. The peak load, crack patterns and load-displacement curves of the experimental tests were simulated accurately using a nonlinear FE prediction model (K. Al-Ghrery et al., 2019).

2.13 Strength deficiency in curved concrete beams

The literature presented regarding curved beam behaviour (Khaleel et al., 2021) comprising investigation done by means of plastic analysis to identify cumulative effect of RC beams subjected to bending, direct shear and torsion done by Badawy et al. in 1977. Set of straight beams and another set of 2.21m radius curved beams casted. All curved beams were provided with nominal reinforcement though transverse rebar and support conditions varied. The same reinforcement provided to the straight beam set with varied flexure, shear and torsion combinations to account for the two yield criteria. Validation of yielding criteria was done by checking with straight beams. As per the conclusions made, approach by plastic analysis is usable for curved beams in which redistribution of internal member forces occur in 2 ways; namely cracking and plastic hinge formation.

Further in view of literature presented regarding curved beam behaviour (Khaleel et al., 2021), Hsu et al. has conducted experiments in 1978 to study post cracking redistribution of flexural and torsional forces to improve its design. Set of 7 nos. 2.74m radius curved beams casted and tested by concentrated point load and fixed support ends. Using conventional design method elastic theory for uncracked concrete structures, two beam specimens were analysed. With the use of elastic theory for uncracked concrete structures, another two beam specimens were analysed ACI Building Code (1971) limiting part of the maximum torsional moment. Using cracked section calculation in elastic method another two beams analysed. The remaining beam was designed as a nominally reinforced controlled beam. Results exhibited that flexural and torsional moment redistribution is large after cracking, traditionally designed beams based on uncracked section (ACI 317-71) exhibited early yielding near supports. Suggestion made in the research to consider cracked section in beam design.

Abul Mansur and Rangan has performed a study for RC curved beams with various design methods. One method is the previously identified collapse load (suggested by Badawy et al.,1977), another is the classical elastic method for uncracked sections and the third which was proposed by authors-limit design. The purpose was to identify strength, failure, reinforcement area effect. As per the results, internal force redistribution occurs in two stages; after cracking and after formation of plastic hinge. In terms of steel usage, Badawy et al.'s method has minimum effect.

2.14 Effect of length of FRP

The effects of CFRP length has been experimented (Ding Jun et al., 2014) with analysing cracking, failure patterns by conducting experimental program for strengthened beams using initial notch. Varying lengths of CFRP, experiments for load bearing capacity were done, where, the crack opening displacements in initial notch also measured. As per the conclusion reached, the influence of CFRP length obvious over carrying capacity and type of failure. Further, finite element method was used to calculate stress at the crack tip, end of CFRP and concrete-CFRP interface. The fine element results also validated the experimental results and theoretical deviances. Finite element and experimental analysis has drawn following conclusions.

Load-bearing capacity for strengthened concrete beams enhances over increase in CFRP length however when CFRP length reached 0.15m in the specimen, increment has halted. Failure noted over length increment at notch tip, notch root and at the end of CFRP. Maximum principal strength in concrete increases till approaching the span of the beam while overstressed region showed the same. Failure mode observed as inclined crack close to CFRP end in one case and smeared crack at root of notching in another case (Ding Jun et al., 2014).

2.15 Durability

Performing durability tests is vital to determine the FRP potential to survive in harsh environments. In research studies upon exposures of wet/dry the change in ultimate load carrying capacity and other structural properties like ductility in FRP tow sheets in tension face was analysed. Even under wet/dry environmental and room temperature conditions, load capacity improvement was clearly seen in both. However lesser improvement was observed under wet/dry environmental conditions. Strength improvement reduction may be attributed to the degradation of the epoxy, which led to the weakening of the bond between the concrete specimens and the FRP sheets (Houssam A. et al., 1997).

Highest load capacity was observed in beams that used epoxy type II, under either environmental condition. Further, it has shown maximum deflection at failure under room temperature exposure and the lowest deflection under wet/dry exposure which concludes that the epoxy selection is imperative in FRP strengthening applications like marine environments (Houssam A. et al., 1997).

2.16 summary

The literature survey recapitulates the use of Carbon fibres due to its very high elastic modulus, strength to weight ratio and comparatively high tensile strength than steel. The diverse forms fabric, plate and rods make its applicability broad.

The literature survey comprehends the consideration that shall be given for load limitations, rational load paths, temperature effects and environmental conditions on FRP systems, loading considerations and also effects of corrosion, when a FRP systems is designed used to increase the member’s strength. Literature references highlighted the resistance of FRP system to all applicable service loads during a fire.

In recap of strengthening experiments, FRP external reinforcement increases the shear and flexure resistance of RC beams in general where shear enhancement in straight beams 10–70% over the control specimens and flexure strengthened beams exhibit an increase in flexural strength of 18-20% percent mostly. Failure modes encounter FRP rupture, debonding in referred literature and it elaborates that influence of debonding failure is higher on initial cracking loads than on stiffness, ductility and the ultimate loads of concrete beams.

In CFRP retrofitting applications outlined in the literature showed that in the crack propagation controlling, placement orientation of CFRP to 45º/135º was effective in the straight beams. CFRP length can increase the ultimate load of the strengthened beam as per findings of research.

The applications of curved beam elements discussed both in-plane and out-of-plane direction of loadings. The in-plane loaded curved beam under varied combinations of torsion, bending and shear were researched in limited numbers. Further, the factor of durability seemed to depend on epoxy selection as well in these FRP applications.

2.17 Further research need

Several research gaps were discovered as a result of the literature review. Despite the fact that numerous studies have been focused on the effect of flexural, shear, torsion, and their combinations acting on FRP strengthened straight RC beams, few of the studies have focussed on the behavior of CFRP strengthened out-of-plane curved RC beams. As a result, it was determined to concentrate on both effects of flexure and shear in curved beams with varying FRP application methods.

CHAPTER 3: EXPERIMENTAL PROGRAM

3.1 Overview

The purpose of this experiment is to investigate the out of plane bending performance of total of six horizontally curved beams with the same dimensions and different strengthening methods. Therefore, two series of curved beams 200mm x 200mm section and curved length of 1.95m were prepared; one series strengthened for flexure (Test series 1) and the other series strengthened for shear (Test series 2).

The flexure strengthened beams were reinforced by 4 nos. T12 bars with R6 shear links at 125mm spacing. Control beam is casted in this series.

The shear strengthened beams prepared with increased bottom reinforcement (2T16) than of flexure strengthened beams and R6 shear links at 125mm spacing. Control beam is casted in this series. The increased flexure r/f will guarantee the beam to fail in shear, which can then be investigated for strength enhancement using CFRP.

Figure 9 illustrates the arrangement of beams test series 1 for flexure strengthening and its control beam in a schematic diagram.

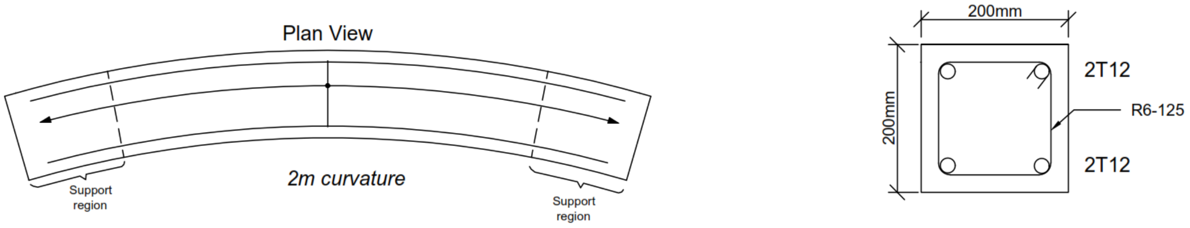

Figure 9: Schematic diagram of specimen of Test series 1

Figure 10 illustrates the arrangement of beam test series 2 for shear strengthening and its control beam in a schematic diagram.

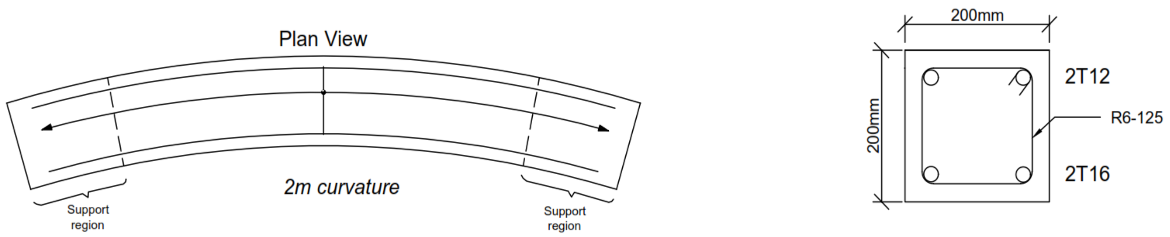

Figure 10: Schematic diagram of specimen of Test series 2

The Test series 1 beam bottom flexure strengthened with 3 nos. 900mm long CFRP plates by NSM method. In order to inspect the effect of clamping of CFRP plates at their ends, CFRP 'U wraps' specimen arranged as per Figure 11.

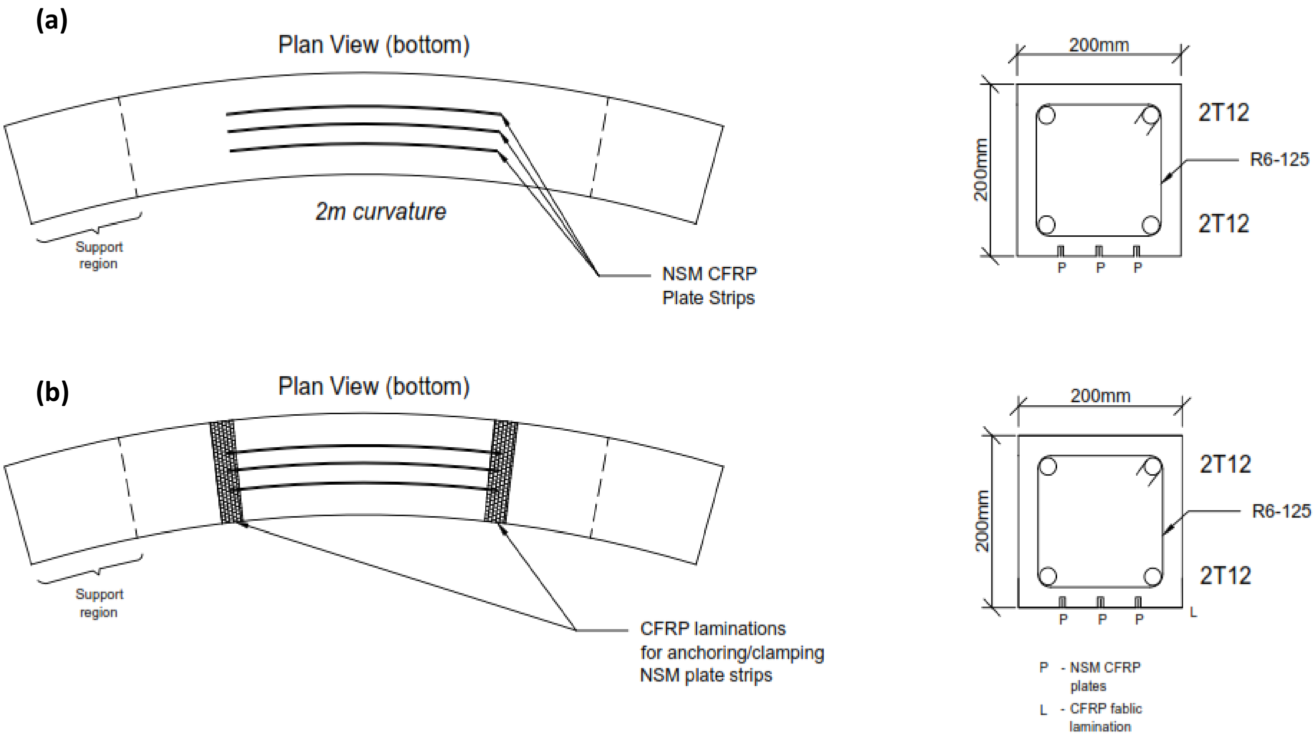

Figure 11: Schematic diagram of specimens of Test series 1- CFRP applications - (a) 3 nos CFRP plates & (b) 3 nos CFRP plates with clamping U-wraps CFRP fabrics

The Test series 2 beams shear strengthened in 2 sides of beam section in the shear zones with uni-directional CFRP fabric. Orientation of the CFRP fabrics selected as 45^{0} /135^{0}. In order to investigate the effect of CFRP enhancement at tentative crack path, the CFRP fabric applied additionally to one specimen as per Figure 12.

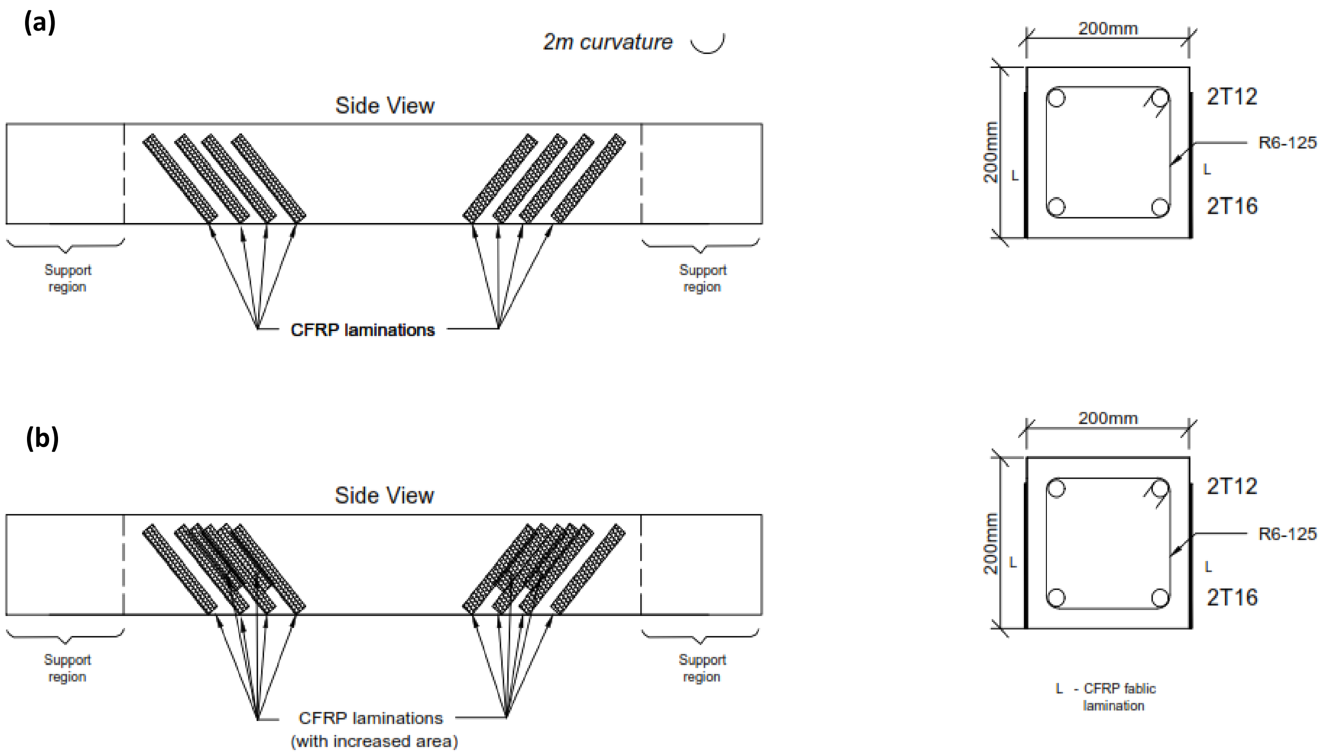

Figure 12: Schematic diagram of specimens of Test series 2- CFRP applications ; (a) CFRP fabric 45/135 at beam sides & (b) CFRP fabric 45/135 at beam sides with extra at inner shear zone

3.2 Material properties

The concrete mix design was done for 30 N/mm^2 compressive strength in 28 days with a standard deviation of 8 N/mm^2 and a 5 % defective rate according to the BRE method (BRE 1992). Concrete test cube specimen of size, 150mm×150 mm ×150 mm was cast to study the compressive strength of concrete which contains two from each batch of concrete (BS 5328). Cubes were cured and tested after 28 days and the average compressive strength was 30 N/mm^2. In all the specimens a clear concrete cover of 25 mm was maintained.

Main steel reinforcement bars are ribbed deformed steel with a tensile strength of 500 N/mm^2 whereas, all stirrups are smooth-surfaced mild steel bars with a tensile strength of 250 N/mm^2.

The manufacturer provided properties of uni-directional carbon fibre Plate strips and fabric are presented in Table 2 and Table 3, respectively. Further, the properties of epoxy-resin adhesive for plates and lamination epoxy-resin for fabric are presented in Table 4 and Table 5, respectively.

Table 2: Properties of carbon fibre Plate strips (X-CALIBUR)

Tensile strength (MPa)	>3000
Modulus of elasticity (GPa)	>165
Nett effective thickness (mm)	1.2
Carbon fibre content	>68%

Table 3: Properties of carbon fibre fabric (X-CALIBUR)

Tensile strength (MPa)	4000
Modulus of elasticity (GPa)	240
Nett effective thickness (mm)	0.166
Elongation at break	2%
Carbon content	95%
Surface mass (g/m^2)	300

Table 4: Properties of the epoxy-resin adhesive (for plates) (X-CALIBUR)

Compressive strength (MPa)	90
Tensile strength (MPa)	23
Flexural strength (MPa)	50
Compressive modulus (GPa)	7
Tensile modulus (GPa)	10
Thermal expansion	33×10^{-6} /^{0}C
Single lap shear strength (MPa)	>18
Water absorption	0.40 %
Tg (DMTA)	>65 ^{0}C

Table 5: Properties of the lamination epoxy-resin (for fabric) (X-CALIBUR)

Tensile strength (MPa)	45
Flexural strength (MPa)	60
Compressive modulus (GPa)	1.67
Viscosity at 20 ^{0}C (cps)	7000
Pot Life at 35 ^{0}C	40 mins
Glass Transition Temperature (^{0}C)	65

3.3 Specimen Preparation

Fabricated Steel formworks were used to obtain the required radius of specimens (Figure 13). Formwork connected using nuts and bolts and uniform width of 200 mm was maintained throughout the beam using stiffener bars welded along the side boards and clamps at mid span. 25 mm thick cover blocks were used in order to maintain the design cover throughout the beam.

Figure 13: Steel formwork and reinforcement cage preparation

The concrete was mixed using a mechanical mixer and subsequently, specimens were cast and labelled. The formworks were removed after 24 hours of casting and curing was carried out by covering the beams using wetted gunny bags (Figure 14). For each mix of concrete, two test cubes were cast and cured. A total of six beam specimens were cast.

Figure 14: Beams cast and cured using gunny bags

3.3.1 Flexure Strengthening of specimens using CFRP plates

The required curved parallel profile of CFRP was marked on the tension face. Diamond cutter was used to open the concrete cover of tension face to make grooves size width of 10 mm, 15 mm deep and length 900 mm [Figure 15(a)]. The weak concrete surface in the end anchoring bonding areas of one beam was ground off using an angle grinder including corners (ACI Committee 440, 2017). After the surface preparation and cleaning the grooves using blower, 1.2mm thick CFRP plates were cut into 15mm width and length of 850 mm using cutter.

For installation, two-part epoxy adhesive was mixed as specified, initially the grooves were filled with the adhesive. An adhesive layer was also applied on the faces of the plates and inserted into the grooves. The plates were held in vertical position until hardened while the excess adhesive was removed [Figure 15(b)].

For the installation of anchorage, fabrics were cut to required U socketing length. The two-part epoxy adhesive was mixed as specified and the first coating was applied over the pasted area of the specimen. Subsequently, the CFRP fabric strips were carefully placed into the proper location and pasted. Finally, the second adhesive coating was applied over carbon fibre strips until adhesive saturate the fabric. The specimens were left to be cured over 7 days.

Figure 15: (a) Cutting grooves; (b) CFRP plate installation

3.3.2 Shear Strengthening of specimens using CFRP fabrics

The concrete surface in the bonding area of CFRP was ground off using an angle grinder. Surface is cleaned out of dust using blower. As specified, the two-part epoxy adhesive was mixed, and the first coating was applied over the ground area of the specimen. Afterward, the CFRP fabric strips were cut and carefully placed in tension direction at the proper location and spacing. Finally, the second coating was applied over carbon fibre strips until adhesive saturate the fabric and left the CFRP to be cured over 7 days. The beam with extra lamination is prepared in the same method (Figure 15).

Figure 16: Surface preparation and CFRP fabric installation

The summary of prepared beam specimen are listed as follows in Table 6.

Table 6: Details of beam specimens

Beam ID	Type	Section dimensions (mm x mm)	Radius of Curvature (m)	Length (m)	Remarks
1-1-CO	Control	200 x 200	2	1.8	4T12
1-2-CO	Control	200 x 200	2	1.8	2T12-T 2T16-B
2-1-FS	NSM CFRP	200 x 200	2	1.8	4T12
2-2-FS	NSM CFRP with end anchorage	200 x 200	2	1.8	4T12
2-1-SS	CFRP laminated at sides	200 x 200	2	1.8	2T12-T 2T16-B
2-2-SS	CFRP laminated extra at sides	200 x 200	2	1.8	2T12-T 2T16-B

3.4 The test setup and instrumentation

The specimens were fixed at supports by clamping the beam to Steel L-Plates resisting twist action (Figure 17). It simulates typical fixed beam to column connection in RC structures. Although a uniform load along the beams should be applied to emulate typical loading conditions of an RC beam, due to the difficulties in applying, managing, and monitoring such a load, the four-point bending method was adopted in accordance with ASTM Standard (D 6415/D 6415M, 2006).

Figure 17: 4 sides clamped at supports

The beam is lifted and placed on supports and clamp it down to strongly grip all four sides of the support section of the specimen to achieve a fixed boundary condition. Two rollers are placed at middle one-third of the effective curved clear span. An I-beam was placed over the two rollers followed by hydraulic jack. Then the loading cell placed over in near touch level to avoid premature loading on the specimen.

Digital dial gauges were placed to measure vertical deformation at the mid-span of the beam either side, prior to load application. A data logger was used to record parameter readings from applied gauges of test setup. The Test setup and instrumentation is shown in Figure 18.

Figure 18: Test setup and instrumentation

The loading on beam was applied gradually and at a constant rate until the ultimate failure occurs. Readings of deflections recorded at each load step. The load at the initial crack, crack propagation and failure modes were recorded. Although this four-point bending setup is more favorable for a shear failure whereas, a three-point bending setup would be more favorable for a flexural failure at the mid-span. The cracks are marked in the order of appearance and observations are noted on failure of fibre or rupture if any.

3.5 Experimental Results

The experimental results of tested flexure strengthened and shear strengthened beams presented indicating ultimate load, first crack load, maximum average deflection and modes of failure (Table 7).

Table 7: Summary results of tested beam specimens

Beam ID	First crack load (kN)	First crack type	Failure load (kN)	Avg. Deflection at failure (mm)	Failure mode
1-1-CO	40.41	Flexure	73.14	18.25	Combined shear and torsional
1-2-CO	45.92	Flexure	75.81	16.00	Combined shear and torsional
2-1-FS	65.13	Flexure	81.99	20.83	Shear
2-2-FS	69.30	Shear	79.32	14.05	Shear
2-1-SS	56.61	Flexure	91.01	17.52	Torsional
2-2-SS	62.45	Shear	98.53	16.37	Shear & intermediate debonding

Further load vs. deflection behaviour and crack propagation were monitored during the testing process of the specimens.

<u>Beam 1-1-CO</u>

The control beam was loaded till failure. Flexural cracks appeared initially at the mid-span bottom at load of 40.41 kN. Shear cracks occurred later and development of further cracks occurred simultaneously at the tension zone, during the occurrence of the shear crack. Figure 19 shows that the flexural cracks widened and slightly propagated towards the compression zone with the increment of loading.

The first shear crack (diagonally) was observed closer to the support area. Thereon the crack widened and diagonally propagated to the 1/3 load point in beam with load increment. Same as the initial diagonal crack, all other shear cracks were also observed to propagate in the same direction. During this widening of shear cracks with the load increase, the beam fails due to shear at a load of 73.1 kN. Figure 20 shows Beam 1-1-CO fails in shear. A torsional component also could have contributed to the shear cracks, which arises due to the curvature of the beam.

Figure 19: Cracks in a Beam 1-1-CO

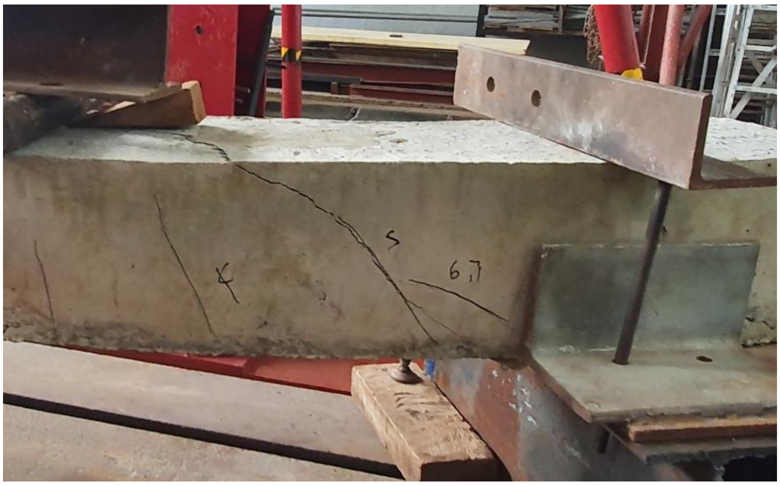

Figure 20: Shear + Torsional failure of Beam 1-1-CO

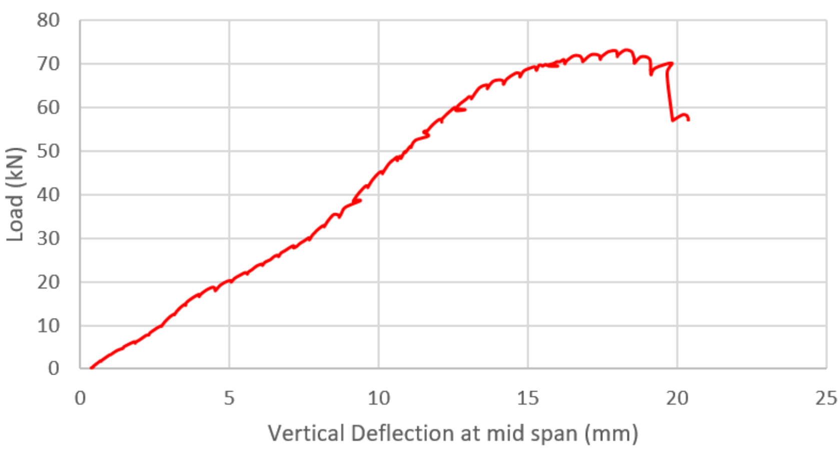

Figure 21: Load vs. Deflection- Beam 1-1-CO

The load vs. deflection response in Figure 23 shows just after 18 kN sudden increase in deflection in the elastic region, but it was not the initial cracking. This may due to sudden jolting at clamped supports due to rotation. After initial cracking at 40.4 kN with appearance of further cracks, the curve shows gradual declination in stiffness until failure. The rotation simultaneously occurs in this region where the failure was shear and torsional, but the graph shows average deflection at mid of beam width at mid span.

Beam 1-2-CO

The control beam which contains higher bottom reinforcement was loaded till failure. Flexural cracks appeared initially at the mid-span bottom at load of 45.92 kN. Shear cracks occurred later and new cracks developed at the tension zone while appearing the shear crack. Figure 22 shows the flexural cracks widened and slightly propagated towards the compression zone with the increment of loading.

The first shear crack (diagonally) was observed closer to the support area. Thereon the crack widened and diagonally propagated to the 1/3 load point in beam with load increment. Same as the initial diagonal crack, all other shear cracks were also observed to propagate in the same direction. During this widening of shear cracks with the load increase, the beam fails due to shear at a load of 75.81 kN. Figure 23 shows Beam 1-2-CO failure by shear. A torsional component also could have contributed to the shear cracks, which arises due to the curvature of the beam.

Figure 22: Cracks in a Beam 1-2-CO

Figure 23: Shear + Torsional failure of Beam 1-2-CO

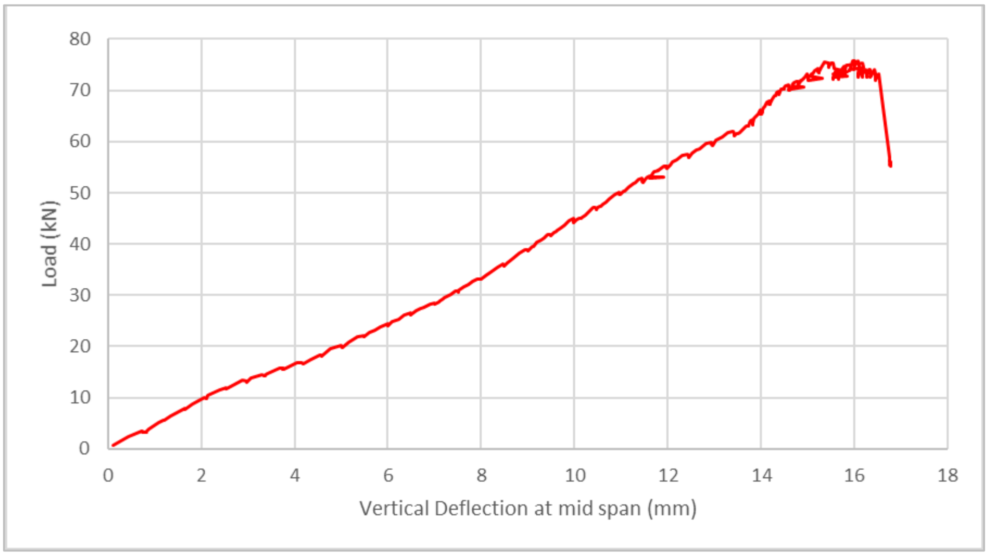

Figure 24: Load vs. Deflection- Beam 1-2-CO

Same as in Beam 1-1-CO, as seen from the load deflection response in Figure 24, after 15 kN abrupt increased deflection that may due to sudden jolting at supports. Thereon the graph shows same initial gradient and minor deviation near 45 kN, signed first cracking. Then rotation simultaneously occurs in this region with new cracks. The failure was shear and torsional, but the graph shows average deflection at mid of beam width at mid span. Lesser deflection of 16mm at failure observed in this beam provided with 2T16 at bottom, compared to beam 1-1-CO.

Beam 2-1-FS

When the NSM CFRP beam is loaded gradually the crack initiation occured at the mid span zone at 65.13 kN load. However this was a single hairline crack which has not propagated upwards. Subsequently new diagonal cracks started to occur close to extreme edge of CFRP plates. All shear cracks observed to propagate and as the load incremented, the shear crack started at plate ends reached the top and the beam ultimately failed by shear at a load of 81.99 kN as shown in Figures 25 & 26.

There was not any debonding occurred in NSM plate strips. However, marked crack no.3 initiated near the plate ends and failure by shear took place in advance.

Figure 25: Cracks in a Beam 2-1-FS

As per the observations; beam has failed in shear and no major flexure cracks appeared, it can be noted that the beam has strengthened satisfactorily for flexure.

Figure 26: Shear failure of Beam 2-1-FS

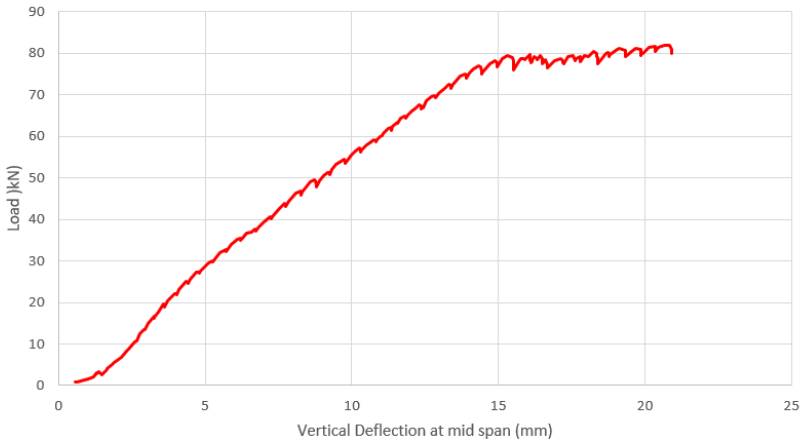

Figure 27: Load vs. Deflection- Beam 2-1-FS

Figure 27 shows a higher stiffness at start of loading than in control beams. After 65 kN with appearance of shear cracks it dominates and the curve shows rapid declination in stiffness until failure by shear. Further, it has deflected significantly without yielding steel reinforcement upto failure at a load of 82 kN.

Beam 2-2-FS

Beam 2-2-FS strengthened with NSM and anchorage CFRP was loaded, the crack initiation occured at the shear zone. Subsequently new diagonal cracks started to occur close to supports. Initial shear cracks were also observed to propagate along edges of the anchorage fabric strip. As the load increases, when this crack reached the top and the strip gets debonded causing the beam to fail at a load of 79.32 kN (Figure 28).

Figure 28: Cracks in a Beam 2-2-FS

The marked crack no.1 near anchorage zone of the beam, initiated and propagated more outwardly than in beam 2-1-FS. Anchorage fabic debonded as shown in Figure 29 when the crack travel along its upper edges. However, any plate strip end debonding not observed.

Figure 29: Shear failure of Beam 2-2-FS & debonding of CFRP fabrics

As per the observations that beam has failed in shear and no flexure cracks appeared, the beam has strengthened satisfactorily for flexure.

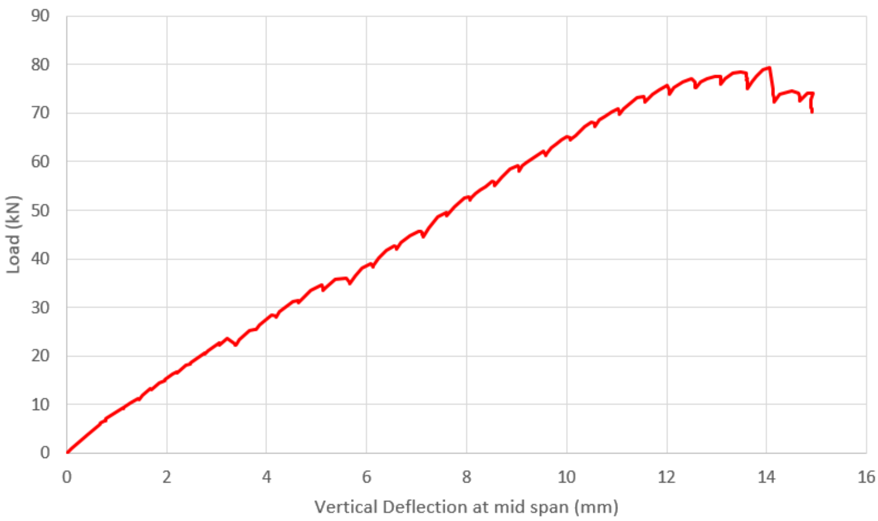

Figure 30: Load vs. Deflection- Beam 2-2-FS

The load vs. deflection response in Figure 30 indicates stable increment in linear region upto 69 kN of initial cracking point. Much lesser deflection of 14.05mm at failure observed in this CFRP anchored beam, compared to beam 2-1-FS.

Beam 2-1-SS

When the $45^0/135^0$ oriented CFRP fabric applied beam is loaded, initially minor flexural cracks at the mid-span appeared. Diagonal crack appeared beyond CFRP zone close to the support, which propagated inwards towards top surface as the load increases. Ultimately failed in torsion at 91.01 kN load indicating a crack at top towards 1/3 point of loading as shown in Figures 31 & 32. Although the beam has failed by torsion, it has been strengthened satisfactorily for shear.

Figure 31: Cracks in a Beam 2-1-SS

Figure 32: Torsional failure of Beam 2-1-SS

There was not any debonding occurred in CFRP fabric. The cracks have not propagated across fabric at any side.

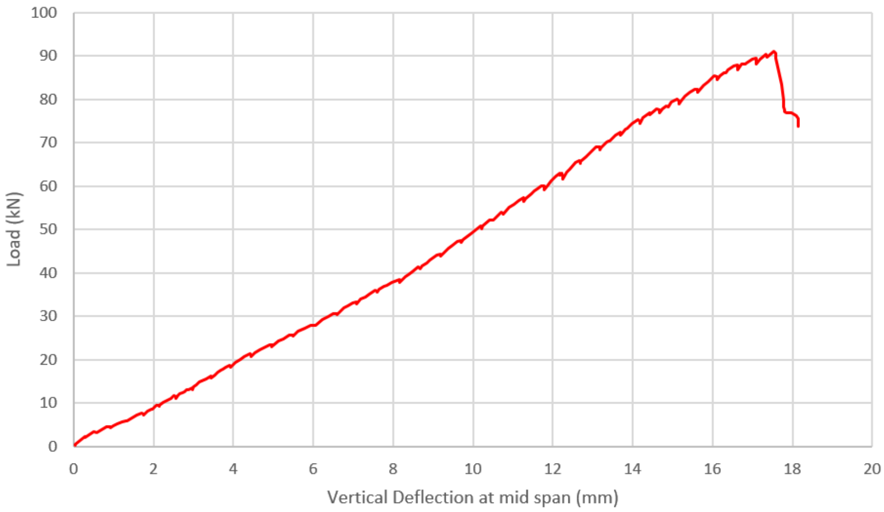

Figure 33: Load vs. Deflection- Beam 2-1-SS

In Figure 33, the curve gradient does only show slight decrement after the initial cracking until failure by torsion. This can be explained by the rotation simultaneously occurs, where the graph shows merely average deflection at mid of beam width at mid span. The deflection of this beam at failure is close to its control beam.

<u>Beam 2-2-SS</u>

When the extra CFRP fabric applied beam is loaded, initially shear crack appeared beyond CFRP zone close to the support. With the load increment, crack propagated through CFRP fabric strips. However, it has not crossed extra CFRP area, but passed above them (Figures 35). Then the outermost fabric got debonded ultimately causing the beam to fail in shear at 98.53 kN load as shown in Figures 34 & 36.

As per the observations, the beam would have been strengthened more satisfactorily for shear than control beam, if CFRP has been placed much closer to supports. Further, the enhancement increased by the extra CFRP application.

Figure 34: Cracks in a Beam 2-2-SS

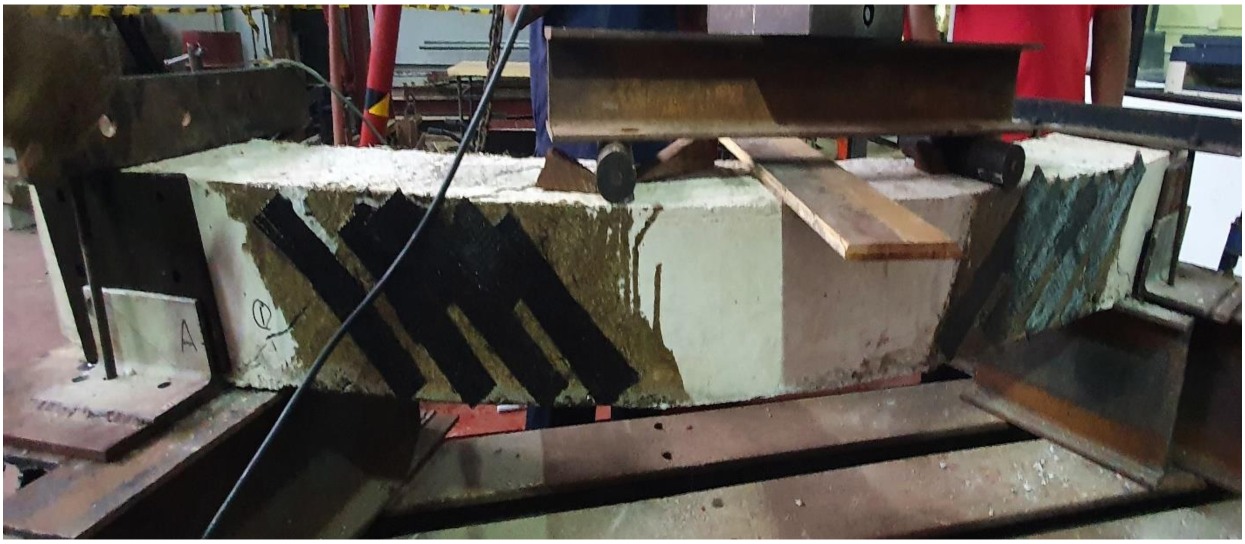

Figure 35: Cracks propagation at CFRP zone in Beam 2-2-SS

Figure 36: Shear crack induced debonding of CFRP in Beam 2-2-SS

Debonding failure occurred in CFRP fabric top zone and it is observed that crack has deviated avoiding FRP area enhanced portion.

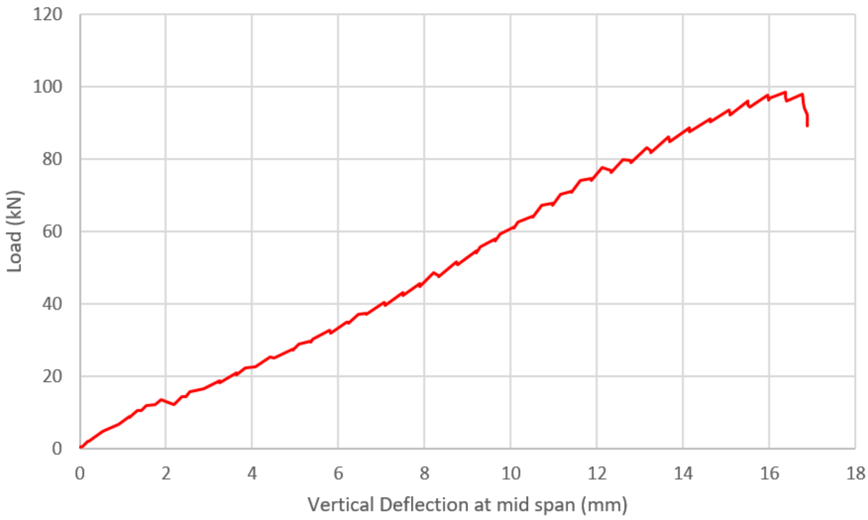

Figure 37: Load vs. Deflection- Beam 2-2-SS

As showed from the load deflection response in Figure 37, after applied load of 17 kN, there is an abrupt increased deflection and regaining same gradient, that may due to sudden jolting at supports. After initial cracking at 62.4 kN, the curve shows gradual declination in stiffness until failure. Since an intermediate debonding happened, the difference in deflection at failure with beam 2-1-SS is minimal.

3.6 Discussion of results

3.6.1 Flexural enhancement

Compared to the control beams, NSM CFRP installed beams show, lesser cracks density. Beam 2-2-FS had no flexure cracks. In addition, initial crack pattern of the control beams was basically consisted of flexural cracks and NSM CFRP beam 2-1-FS showed 61% increment of initial cracking load. Although the flexure failure modes did not witness due to the nature of high curvature beams tested, it can be noted that the flexural strength has been significantly enhanced.

Further, crack pattern of the Beam 2-2-FS indicated that cracking in the direction of CFRP plate corners is restrained with the use of end anchoring CFRP. However, it has not contributed for any difference to degree of shear capacity enhancement as per failure load results. However ultimate load carrying capacity of RC beams 2-1-FS and 2-2-FS were increased by 12.1% and 8.4% respectively.

3.6.1.1 Comparison of deflections

The Load vs. Deflection relationship of tested specimens for flexure strengthening are shown in Figure 38.

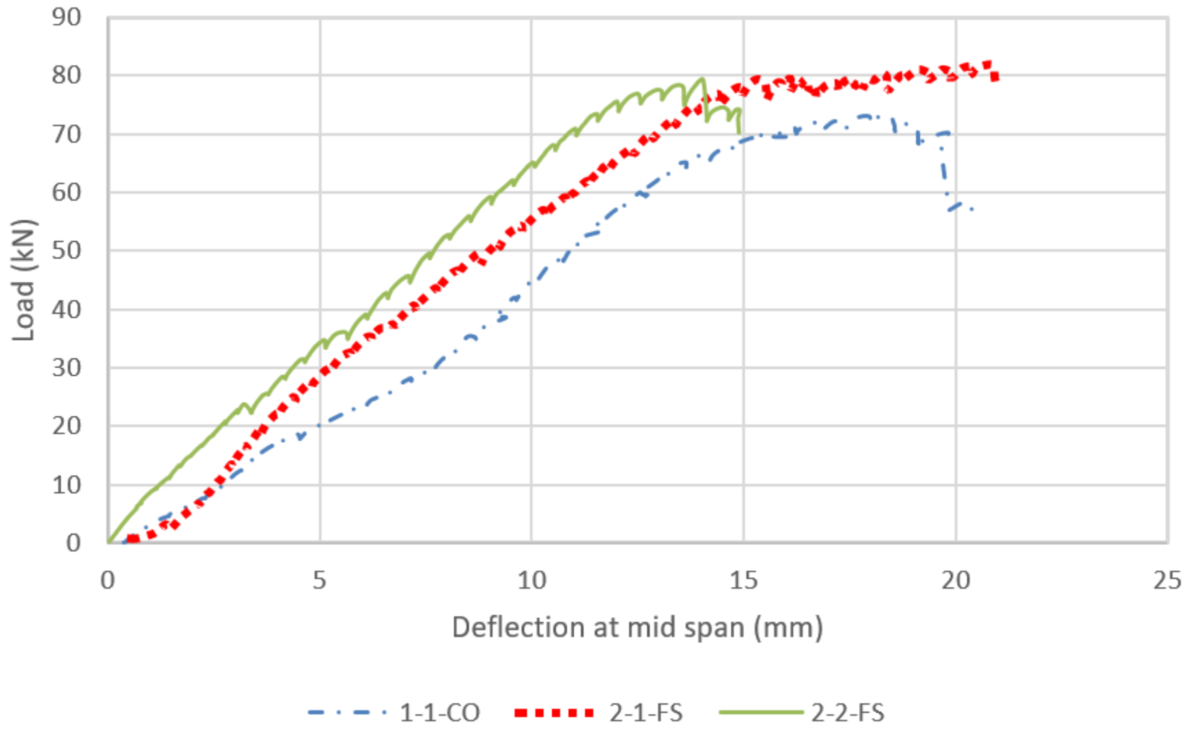

Figure 38: Load vs. deflection- Beams retrofitted for flexure

A 23% reduction of deflection observed in CFRP plate end clamped beam. The beam having only CFRP plates has not shown such reduction. This may be due to premature bond failure during cracking. The slope of the graphs for CFRP strengthened beams are greater than that of control beams, which indicate an increase in the stiffness due to the application of CFRP. The elastic zone of flexure strengthened beams in Figure 38 are more stable than in control beam.

3.6.2 Shear enhancement

Compared to the control beams, CFRP strengthened 2-1-SS and 2-2-SS beams shows ultimate load carrying capacity increment of 20 % and 30% respectively. Therefore, CFRP retrofitting in beam's inner upper section of shear span has contributed additional 10% increment of its carrying capacity. Beam 2-1-SS and 2-2-SS show 23.2% and 36% increment of initial cracking load respectively. Flexure cracks are almost none after retrofitting. These beams were expected to be failed under shear (higher bottom reinforcement) and in all 3 beams exhibited major shear zone cracks and failed by shear or torsion.

3.6.2.1 Comparison of deflections

The Load vs. Deflection relationship of tested specimens for flexure strengthening are shown in Figure 39.

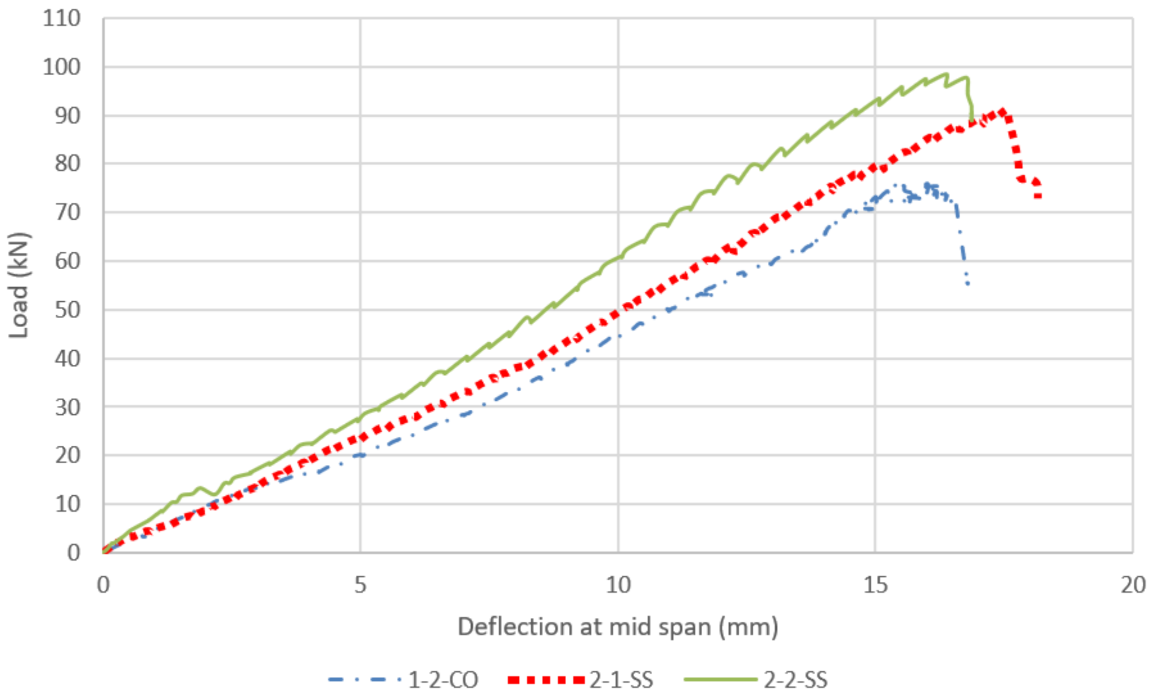

Figure 39: Load vs. deflection- Beams retrofitted for shear

Deflection of beams at failure is almost similar for all 3 beams which indicate CFRP fabric application has minor effect over bending. It can be observed that the slopes of the graphs for CFRP strengthened beams are greater than that of control beams, which indicates an increase in the stiffness due to the application of CFRP fabrics.

In beams 2-1-SS and 2-2-SS if the side laminations fixed nearer to supports, the only cracks appeared could have not propagated up and failure load may increase further. However, as seen from Figure 39, FRP area addition in the inner shear zone contributed more carrying capacity at a lesser deflection.

CHAPTER 4: THEORETICAL ANALYSIS

4.1 Preliminary theoretical calculation for experimental program

Preliminary calculation done for the purpose of prediction of flexural and shear capacities of the curved beams test specimens is presented. The responses expressions for shear and flexure of the horizontally curved beam element subjected to out-of-plane, four-point bending loading are included.

The testing of curved beam specimens carried out using four-point bending loading in order to approximate actual loading in a building, where uniformly distributed loading is practically encountered by the beam through slab. Three-point bending loading method does not represent this distributed loading and bending moment and shear force profiles also differ. Further, applying udl in laboratory is practically difficult for a curved beam. Therefore, the four-point bending method is adopted as the suitable method of loading to make viable recommendations by the research.

4.2 General response expressions of a horizontally curved beam under out-of-plane loads

The general response expressions for concentrated and distributed, forces and moments loading shown in Figure 40 have computed by Pilkey, (2005).

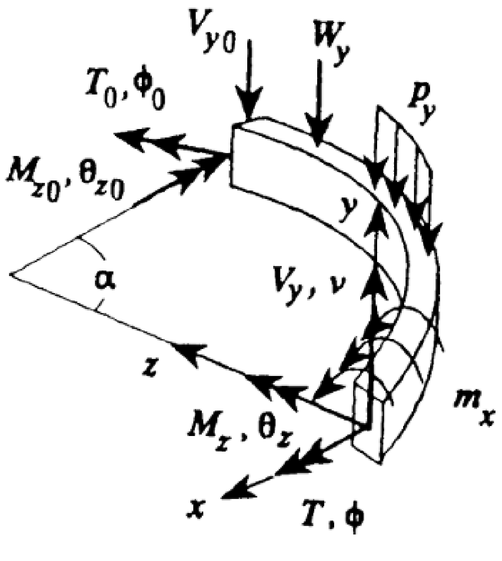

Figure 40: Loading functions and responses of horizontally curved, out of plane loaded beams (Pilkey, 2005)

Following six general response expressions can be used to find the internal forces per single loading. The initial boundary conditions of each degree of freedom is used for the first 3 expressions. In four-point bending, each point load at one third locations applied and principal of superposition used to find the final results.

Angle of twist:

$$\emptyset = \emptyset_0 \cos\alpha + \theta_{z0} \sin\alpha - V_{y0}\lambda_1 R^2 + \frac{1}{2} M_{z0}\lambda_1 R\alpha \sin\alpha + T_0\left(\frac{R}{GJ}\lambda_5 - \frac{R}{EI_z}\lambda_2\right) + F_{\emptyset} \tag{1}$$

Deflection:

$$\upsilon = -\phi_0 R(\cos\alpha - 1) + \upsilon_0 + \Theta_{z0} R \sin\alpha + V_{y0}\left(\frac{R^3}{GJ}\lambda_4 - \frac{R^3}{EI_z}\lambda_2\right) + M_{z0}\left(\frac{R^2\alpha}{2EI_z}\sin\alpha - \frac{R^2}{GJ}\lambda_3\right) - T_0\lambda_1 R^2\lambda_2 + F_\upsilon \tag{2}$$

Slope:

$$\Theta_z = -\phi_0 \sin\alpha + \Theta_{z0}\cos\alpha + V_{z0}\left(\frac{R^2}{GJ}\lambda_3 - \frac{R^2\alpha}{2EI_z}\sin\alpha\right) + M_{z0}\left(\frac{R}{EI_z}\lambda_5 - \frac{R}{GJ}\lambda_2\right) - \frac{1}{2}T_0\lambda_1 R\alpha\sin\alpha + F_{\Theta z} \tag{3}$$

Shear force:

$$V_y = V_{y0} + F_{vy} \tag{4}$$

Bending moment:

$$M_z = -V_{y0} R \sin\alpha + M_{z0}\cos\alpha - T_0 \sin\alpha + F_{Mz} \tag{5}$$

Torque:

$$T = V_{y0}(\cos\alpha - 1) + M_{z0}\sin\alpha + T_0\cos\alpha + F_T \tag{6}$$

Notation used for the expressions of all loading functions are as follows.

E	-	Modulus of elasticity
G	-	Shear modulus of elasticity
R	-	Radius of arc

J	-	Torsional constant
I_z	-	Moment of inertia about the z-axis
λ_1	-	$\frac{1}{GJ} + \frac{1}{EI_z}$
λ_2	-	$\frac{1}{2}(\sin\alpha - \alpha\cos\alpha)$
λ_3	-	$\frac{1}{2}(2 - 2\cos\alpha - \alpha\sin\alpha)$
λ_4	-	$\frac{1}{2}(2\alpha + \alpha\cos\alpha - 3\sin\alpha)$
λ_5	-	$\frac{1}{2}(\alpha\cos\alpha + \sin\alpha)$

Loading functions $F_{\emptyset}, F_v, F_{\Theta z}, F_{vy}, F_{Mz}$ and F_T in above six equations are defined for an applied concentrated load as below, with the notation in Figure 41.

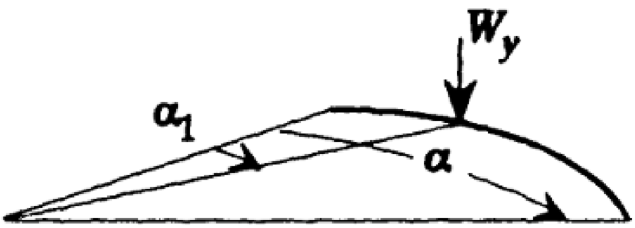

$$< \alpha - \alpha_1 >^0 \quad - \quad \begin{cases} 0 & \alpha < \alpha_1 \\ 1 & \alpha \geq \alpha_1 \end{cases}$$

$$< \alpha - \alpha_1 > \quad - \quad \begin{cases} 0 & \alpha < \alpha_1 \\ (\alpha - \alpha_1) & \alpha \geq \alpha_1 \end{cases}$$

Figure 41: Notation for concentrated vertical load on a horizontally curved beam (Pilkey, 2005)

$$F_\phi = \frac{W_y \lambda_1 R^2}{2}[\sin < \alpha - \alpha_1 > - < \alpha - \alpha_1 > \cos(\alpha - \alpha_1)] \tag{7}$$

$$F_v = -\frac{W_y R^3}{2}\left\{\frac{1}{GJ}[2 < \alpha - \alpha_1 > + < \alpha - \alpha_1 > \cos(\alpha - \alpha_1) - 3\sin < \alpha - \alpha_1 >] - \frac{1}{EI_z}[\sin < \alpha - \alpha_1 > - < \alpha - \alpha_1 > \cos(\alpha - \alpha_1)]\right\} \tag{8}$$

$$F_{\theta z} = \frac{W_y R^2}{2}\left\{\frac{1}{EI_z}[< \alpha - \alpha_1 > \sin(\alpha - \alpha_1)] - \frac{1}{GJ}[2 < \alpha - \alpha_1 >^0 - 2 < \alpha - \alpha_1 >^0 \cos(\alpha - \alpha_1) - < \alpha - \alpha_1 > \sin(\alpha - \alpha_1)]\right\} \quad 9$$

$$F_{vy} = -W_y \quad 10$$

$$F_{Mz} = W_y R \sin < \alpha - \alpha_1 > \quad 11$$

$$F_T = W_y R(< \alpha - \alpha_1 >^0 \cos(\alpha - \alpha_1) - < \alpha - \alpha_1 >^0) \quad 12$$

4.3 Determination of flexural and shear capacities of the beams

Flexural and shear capacities of the beam series 1 and 2 were predicted theoretically based on the Euro standard (BS EN 1992-1-1, 2004).

4.3.1 Flexural capacities of RC beams without CFRP external reinforcement

The ultimate moment of resistance of a rectangular section is given by Equation 13 in Euro standard (BS EN 1992-1-1, 2004).

$$M_1 = 0.25092 f_{ck} b d^2 \quad 13$$

In consideration of the material properties, experimental setup and quality of casting, the safety factors of following relevant equations in Euro standard (BS EN 1992-1-1, 2004) are removed. The modified Equations are shown below. The relationship between the applied moment and the tensile reinforcement is given by Equation 14.

$$M = A_s f_{yk} z \quad 14$$

where,

$$z = \frac{d}{2}\left[1 + \sqrt{1 - \frac{2.353M}{f_{ck} b d^2}}\right] \quad 15$$

Substituting this z to Equation 14 and subsequently simplifying, Equation 16 for the ultimate moment of resistance can be derived.

$$M_2 = A_s f_{yk} d - 0.58825 \frac{A_s^2 f_{yk}^2}{b f_{ck}} \qquad 16$$

Then, the ultimate flexural capacity is taken as the minimum of M_1 and M_2.

4.3.2 Moment resistance of an uncracked beam section at crack initiation

Moment resistance of the uncracked section can be derived from the linear triangular stress block of tension and compression zone shown in Figure 42 (Mosley, 2007).

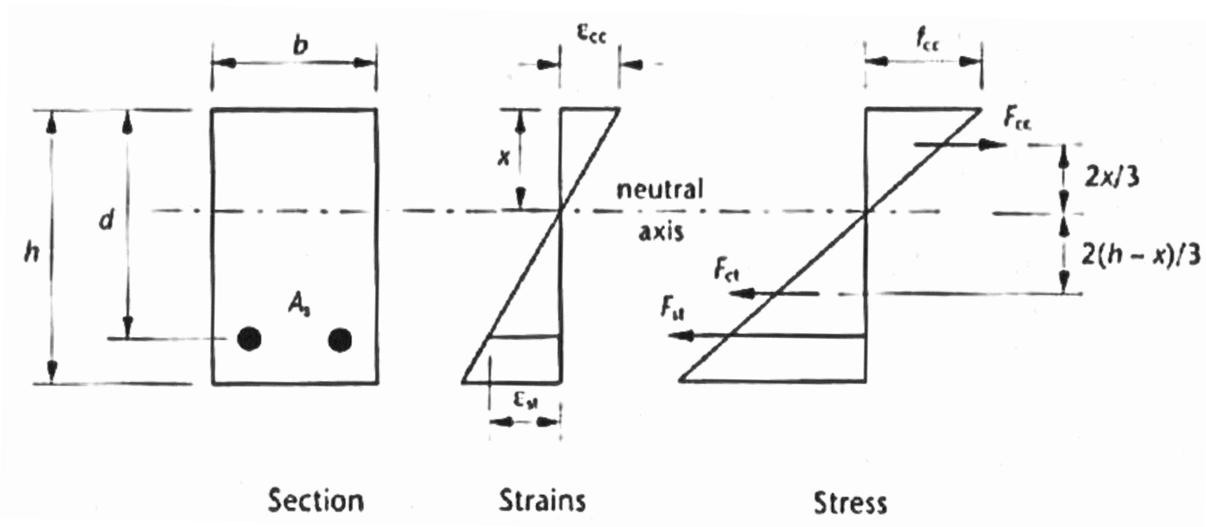

Figure 42: Triangular stress block for uncracked section

Moment resistance given by the section is given by Equation 17.

$$M = F_{st}\left(d - \frac{x}{3}\right) + F_{ct}\left[\frac{2}{3}x + \frac{2}{3}(h - x)\right] \qquad 17$$

Where,

$$x = \frac{h + 2\alpha_c A_s \frac{d}{bh}}{2 + 2\alpha_c \frac{A_s}{bh}} \qquad 18$$

$$\alpha_c = \frac{E_s}{E_c}$$

A_s - area of the tensile reinforcement

From the linear proportions of strain diagram stresses can be derived as follows.

$$f_{ct} = E_c \varepsilon_{ct} \qquad (19)$$

where, f_{ct} can be considered as 3 N/mm^2

$$f_{st} = \frac{(d-x)}{(h-x)} \alpha_c f_{ct} \qquad (20)$$

4.3.3 Shear capacities of RC beams without CFRP installation

4.3.3.1 Shear capacity with shear links

With shear links, failure can be in the way of compression of an imagined diagonal concrete strut or it can be the tensile failure of the member.

For tensile failure, the shear force is given by Equation 21 (BS EN 1992-1-1, 2004).

$$V_{Rd,s} = \frac{A_s}{s} z f_y \cot\theta \qquad (21)$$

Where,

A_s is the area of the tensile reinforcement

s is the spacing of stirrups

$z = d - d'$

f_y is the tensile strength of stirrups

Cot θ can vary between 1 and 2.5 depending on the magnitude of the shear force. Hence, for the maximum resistance of shear links, it can be taken as 2.5.

For compressive failure, the shear force is given by,

$$V_{Rd,max} = \alpha_{cw} b_w z v_1 f_{ck} / (\cot\theta + \tan\theta) \qquad (22)$$

Where,

$\alpha_{cw} = 1$

$v_1 = 0.6 \left[1 - \frac{f_{ck}}{250}\right]$

4.3.4 Flexural capacity enhancement from NSM FRP plates

The guidance provided for externally bonded FRP systems by standard guide published by technical committees (ACI Committee 440, 2017), which were developed for planning, design and inspecting work in construction. As per the distribution at equilibrium of the section and notation given in Figure 43 flexural strength enhancement by FRP is given by Equation 23 below.

$$M_{nf} = A_s f_{fe}\left(d_f - \frac{\beta_1 c}{2}\right) \quad (23)$$

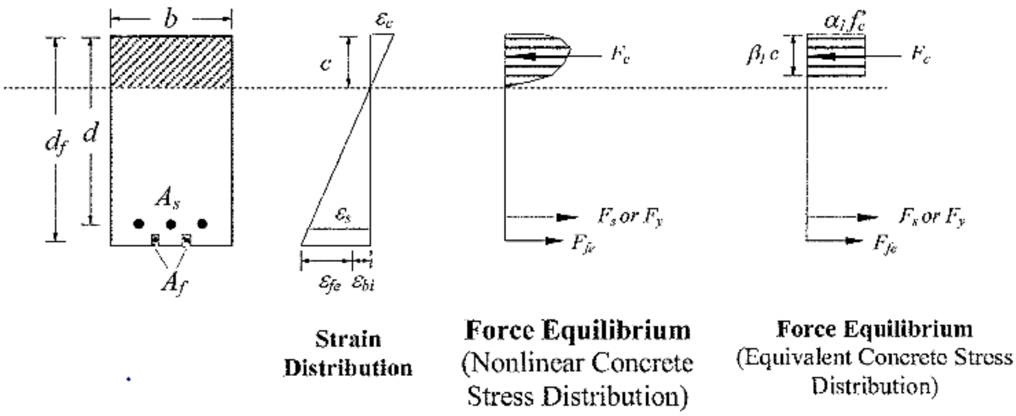

Figure 43: Internal stress and strain with NSM FRP at ULS flexure (ACI Committee 440, 2017)

By Hook's law,

$$f_{fe} = E_f \varepsilon_{fe} \quad (24)$$

$$f_s = E_s \varepsilon_s \le f_y \quad (25)$$

Where to find effective strain level of FRP,

$$\varepsilon_{fe} = \left(\frac{d_f - c}{c}\right) - \varepsilon_{bi} \le \kappa_m \varepsilon_{fd} \quad (26)$$

Using cracked section analysis,

$$\varepsilon_{bi} = \frac{M_{DL}(d_f - kd)}{I_{cr}E_c} \quad 27$$

Stain in steel reinforcement can be calculated as,

$$\varepsilon_s = (\varepsilon_{fe} + \varepsilon_{bi})\left(\frac{d-c}{d_f - c}\right) \quad 28$$

To calculate depth to neutral axis c, at equilibrium,

$$c = \frac{A_s f_s + A_f f_{fe}}{\alpha_1 f_c' \beta_1 b} \quad 29$$

Where,

$$\beta_1 = \frac{4\varepsilon_c' - \varepsilon_c}{6\varepsilon_c' - 2\varepsilon_c} \quad 30$$

$$\alpha_1 = \frac{3\varepsilon_c'\varepsilon_c - \varepsilon_c^2}{3\beta_1\varepsilon_c'^2} \quad 31$$

$$\varepsilon_c' = \frac{1.7 f_c'}{E_c} \quad 32$$

$$\varepsilon_c = (\varepsilon_{fd} + \varepsilon_{bi})\left(\frac{c}{d_f - c}\right) \quad 33$$

4.3.5 Shear capacity enhancement from FRP side laminations

The guidance provided for externally bonded FRP systems by standard guide published by technical committees (ACI Committee 440, 2017), prescribes expression for shear strength enhancement by laminating FRP given by Equation 24, as per variables and dimensions notated in Figure 44.

$$V_f = \frac{A_{fv} f_{fe}(\sin\alpha + \cos\alpha) d_f}{s_f} \quad 34$$

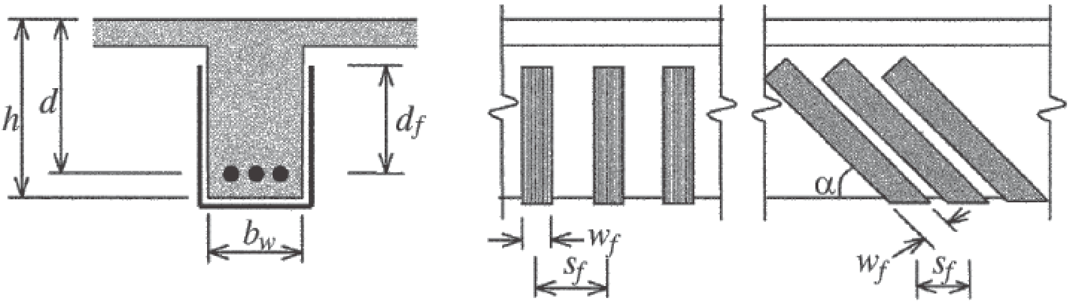

Figure 44: Dimensions and variables for calculation for FRP laminates shear strengthening (ACI Committee 440, 2017)

For a rectangular cross section,

$$A_{fv} = 2nt_f w_f \quad 35$$

Where,

t_f - FRP sheet thickness

By Hook's law

$$f_{fe} = E_f \varepsilon_{fe} \quad 36$$

For completely wrapped members

$$\varepsilon_{fe} = 0.004 \le 0.75\varepsilon_{fu} \quad 37$$

Where,

ε_{fu} is the rupture strain of the FRP and E_f is Young's modulus of FRP.

For U-wraps and side bonding,

$$\varepsilon_{fe} = \kappa_v \varepsilon_{fu} \le 0.004 \quad 38$$

κ_v is the bond-reduction coefficient which is a function of the strength of concrete, wrapping scheme and the active bond length and is determined using Equations 29, 30,31 and 32.

$$\kappa_v = \frac{k_1 k_2 L_e}{11900\varepsilon_{fu}} \le 0.75 \quad 39$$

$$k_1 = \left(\frac{f_c'}{27}\right)^{2/3} \quad 40$$

$$k_2 = \begin{cases} \frac{d_{fv} - L_e}{d_{fv}}, & for\ U - wraps \\ \frac{d_{fv} - 2L_e}{d_{fv}}, & for\ side\ bonding \end{cases} \quad 41$$

$$L_e = \frac{23300}{\left(nt_f E_f\right)^{0.58}} \quad 42$$

4.3.6 Transverse FRP U-wrap anchorage at ends of NSM FRP plates

The anchorage bonding applications considered in guide (ACI Committee 440, 2017) including for seismic loads. The FRP wrap reinforcement area is given by Equation 33.

$$A_{fanchor} = \frac{(A_f f_{fe})_{longitudinal}}{(E_f \kappa_v \varepsilon_{fu})_{anchor}} \quad 43$$

Where,

A_f is the longitudinal FRP area

f_{fe} calculated by Equation 26 above

κ_v is the bond-reduction coefficient

ε_{fu} is the rupture strain and E_f is Young's modulus of FRP.

In addition, length of wrap anchorage FRP should satisfy Equation 34.

$$l_{d,E} \geq l_0 + l_{df} \quad 44$$

For adequate anchorage of FRP, effective design stain ε_{fd} should satisfy,

$$\varepsilon_{fd} \leq \min(0.9\varepsilon_{fu}, C_E \varepsilon_{fu}) \quad 45$$

4.4. Comparison of experimental results with theoretical predictions

The experimental results were compared with theoretical results obtained from Eurocode 2 and ACI 440.2R-17 and presented in Table 8 and 9 for series 1 and 2 respectively.

Table 8: Series 1- Experimental vs. theoretical results comparison

	Actual			**Theoretical prediction**			**Difference %**
Specimen ID	**1-1-CO**	**2-1-FS**	**2-2-FS**	**1-1-CO**	**2-1-FS**	**2-2-FS**	
Moment Capacity (kNm)	-	-	-	16.93	22.17	23.82	-
Shear Capacity (kN)	-	-	-	30.16	30.16	30.16	-
First cracking load (kN)	40.41	65.13	69.30	35.10	*	*	1-1-CO: -15.1
Failure Load (kN)	73.14	81.99	79.32	81.20	93.64	96.50	1-1-CO: 9.9 2-1-FS: 12.4 2-2-FS: 17.8
Failure Mode	shear and torsional	Shear	Shear	Shear	Shear	Shear	-
CFRP Flexural enhancement (kN)	N/A	8.85	10.81	N/A	12.44	15.30	2-1-FS: 28.8 2-2-FS: 29.3

* Accurate calculation is difficult due to cut grooves in beam bottom

Table 9: Series 2- Experimental vs. theoretical results comparison

	Actual			**Theoretical prediction**			**Difference %**
Specimen ID	**1-2-CO**	**2-1-SS**	**2-2-SS**	**1-2-CO**	**2-1-SS**	**2-2-SS**	
Moment Capacity (kNm)	-	-	-	27.61	27.61	27.61	-
Shear Capacity (kN)	-	-	-	29.21	52.75	57.71	
First cracking load (kN)	45.92	56.61	62.45	37.90	*	*	1-2-CO: -21.1
Failure Load (kN)	75.81	91.01	98.53	78.7	125.27	130.88	1-2-CO: 3.6 2-1-SS: 27.3 2-2-SS: 24.7
Failure Mode	shear and torsional	Torsional	Shear & intermediate debonding	Shear	Shear	Shear	-
CFRP Shear enhancement (kN)	N/A	15.2	22.72	N/A	23.54	28.50	2-1-SS: 35.4 2-2-SS: 20.3

* Prediction require complex calculation due to curved profile of FRP

As per the comparison in Table 8, the load carrying capacities has a reduced by 9.9%, 12.4% and 17.8% of their predicted values, which may due to torsional stress additionally induced. Due to the curvature and torsional effects, the predicted capacity enhancement is 28.8% and 29.3% less than predicted values by ACI 440.2R-17. Further, the actual initial cracking load of control beam is 15.1% higher than the predicted value, since the visibility of crack by naked eye can be delayed practically than the exact point of crack initiation.

In series 2 beams, the load carrying capacities has a reduced by 3.6%, 27.3% and 24.7% of their predicted values, which may due to torsional stress additionally induced as per the comparison in Table 9. Due to the curvature, intermediate debonding occurred and torsional effects, the predicted capacity enhancement is 35.4% and 20.3% less than predicted values. Further, the actual initial cracking load of control beam is 21.1% higher than the predicted value, which can be due to delay to identify the point of initiation of micro crack.

CHAPTER 5: CONCLUSIONS AND RECOMMENDATIONS

5.1 Conclusions

From the observations on the behavior of the strengthened curved beams during testing loading history, ultimate failure load, modes of failure and crack pattern, some key points can be deduced and summarised regarding effectiveness of CFRP strengthening.

1. Tested Curved beam of 2m radius of curvature NSM CFRP beam 2-1-FS showed 61% increment of initial cracking load and beam 2-2-FS had no flexure cracks. With NSM method flexural strength has enhanced. End anchored CFRP fabric provide additional flexure strength and reduce deflection by 23%.

2. Ultimate load carrying capacity of NSM CFRP retrofitted beams 2-1-FS and 2-2-FS were increased by 12.1% and 8.4% respectively. NSM CFRP retrofitting has influence over ultimate load carrying capacity even at failure by shear.

3. Compared to the control beams, NSM CFRP retrofitted beams showed, lesser cracks density and reduced crack widths. Propagation of the crack which was in the direction of NSM CFRP plate corners is restrained with the use of end anchored CFRP. However, its effect over shear capacity enhancement is insignificant.

4. The experimental flexural enhancements are 28.8% and 29.3% less than the theoretically predicted values by ACI 440.2R-17 guide, respectively for NSM CFRP only and end anchored beams, which may have occurred due to the contribution of additionally induced torsional stresses.

5. Ultimate load carrying capacity of 45º/135º oriented CFRP fabric installed curved beams 2-1-SS and 2-2-SS were increased by 20 % and 30% respectively. The influence of CFRP retrofitting is 10% higher when the area of CFRP application is increased in inner shear span.

6. Shear strengthened beams showed higher stiffness than control beams. Nevertheless, failure mode is commonly shear or torsion or shear induced rupture in CFRP or combination of any of them.

7. The experimental shear enhancements are 35.4% and 20.3% less than the theoretically predicted values by ACI 440.2R-17 guide, respectively for side laminated and extra side laminated beams. The intermediate debonding and induced additional torsional stresses may have caused this capacity reduction.

5.2 Recommendations

1. Curved beams of different depths can be used to evaluate on the CFRP retrofitting enhancement of flexure and shear carrying capacity.
2. Intermediately cracked beams (before failure) can be retrofitted after CFRP installation to analyse the enhancement of carrying capacity. It will resemble a real time retrofitting scenario.
3. Research areas are open for use of natural fibres like bamboo or modified natural fibre to be mounted in structural elements in future research to assess degree of usability as a cost effective and sustainable retrofitting technique.

REFERENCES

ACI Committee 318, 2014. Building Code Requirements for Structural Concrete, American Concrete Institute. doi:10.14359/51716937

ACI Committee 440, 2017. ACI 440.2R-17 Guide for the Design and Construction of Externally Bonded FRP Systems for Strengthening Concrete Structures, Guide for the Design and Construction of Externally Bonded FRP Systems for Strengthening Concrete Structures.

Ali, N., Samad, A., Mohamad, N. and Jayaprakash, J. (2013). Shear Behaviour of Pre-cracked Continuous Beam Repaired using Externally Bonded CFRP Strips. *Procedia Engineering*, 53, 129-144. doi:10.1016/j.proeng.2013.02.019

Al-Ghrery, K., Kalfat, R., Oukaili, N., Al-Mosawe, A. and Al-Mahaidi, R. (2019). Finite Element Modelling of Curved Soffit Reinforced Concrete Beams Strengthened with Fibre Reinforced Polymer. *Seventh Asia-Pacific Conference on FRP in Structures*

Alkhrdaji, T. (2015). Strengthening of Concrete Structures Using FRP Composites, *Structure Magazine*, 18-20.

Babu, A. and Bhattacharya, A. (2020). Review on Use of Carbon Fibre (Reinforced Plastics) in Automotive Sector. *Journal of Critical Reviews*. 7, 679-684. doi:10.31838/jcr.07.01.132

Balamuralikrishnan, R., and C. Antony Jeyasehar. (2009). Flexural Behavior of RC Beams Strengthened with Carbon Fibre Reinforced Polymer (CFRP) Fabrics. *The Open Civil Engineering Journal 3*, 102-109. doi:https:10.2174/1874149500903010102

Bhatt, P. and Goe, A. (2017). Carbon Fibres: Production, Properties and Potential Use. *Material Science Research India*. 14(1), 52-57. doi:10.13005/msri/140109

Breveglieri, M., Aprile, A. and Barros, J. (2015). Embedded Through-Section shear strengthening technique using steel and CFRP bars in RC beams of different percentage of existing stirrups. *Composite Structures*. 126, 101-113. doi:10.1016/j.compstruct.2015.02.025

Burke, P., Bisby, L. & Green, M. (2013). Effects of elevated temperature on near surface mounted and externally bonded FRP strengthening systems for concrete. *Cement and Concrete Composites*. 35. 190–199. doi:10.1016/j.cemconcomp.2012.10.003

Cao, S.Y., Chen, J.F., Teng, J.G., Hao, Z., Chen, J., 2005. Debonding in RC Beams Shear Strengthened with Complete FRP Wraps. *Journal of Composites for Construction* 9, 417–428.

Damian I. K. (2000). Testing of Full-Size Reinforced Concrete Beams Strengthened with FRP Composites: Experimental Results and Design Methods Verification. *Report no.FHWA-OR-RD-00-19.*

Diab, H.M.A., Abdelaleem, T., Rashwan, M.M.M., 2020. Moment redistribution and flexural performance of RC continuous T-beams strengthened with NSM FRP or steel bars. *Structures* 28, 1516–1538. doi:10.1016/j.istruc.2020.09.003

Ding, J., Wang, F., Huang, X. and Chen, S. (2014). The Effect of CFRP Length on The Failure Mode of Strengthened concrete Beams. *Polymers 6.6*, 1705-1726.

Fathelbab, F.A., M.S. Ramadan, and A. Al-Tantawy. (2011). Finite Element Modeling Of Strengthened Simple Beams Using FRP Techniques: A Parametric Study. *Concrete Research Letters (2)*. 2 ,228-240.

Gao, B., Kim, J. and Leung, C. (2006). Strengthening efficiency of taper ended FRP strips bonded to RC beams. *Composite science and technology*. 66, 2257-2264.

Garden, H.N., and Hollaway, L.C. . (1998). An experimental study of the influence of plate end anchorage of carbon fibre composite plates used to strengthen reinforced concrete beams. *Composite Structures*. 42 (2), 175-88.

Grelle, S. v., Sneed, L.H., 2013. Review of Anchorage Systems for Externally Bonded FRP Laminates. International Journal of Concrete Structures and Materials 7, 17–33.

Hayes B.J. (1985). Experiences of Non-Aerospace Application of CFRPs in Europe. Carbon Fibres and Their Composites. Springer, Berlin, Heidelberg. pp 253-260. doi:10.1007/978-3-642-70725-4_16

Houssam A.T. (1997). The Durability characteristics of concrete beams externally bonded with FRP composite sheets. 351-358.

Hawileh, R., Nawaz, W., Abdalla, J. and Saqan, E. (2015). Effect of flexural CFRP sheets on shear resistance of reinforced concrete beams. *Composite Structures*. 122, 468-476.

Hui, L.L., Bashar, S., Mohammed, M.S., Liew, M.M.A. and WahabAminAl-Fakih (2020). Bond behaviour of CFRP-strengthened ECC using Response Surface Methodology (RSM). *Case Studies in Construction Materials. Volume 12.*

Kahandawaarachchi, K., Gamage, J, C, P, H., Chandrathilaka, E.R.K., 2019. Bond Performance of Carbon Fibre Reinforced Polymer (CFRP) Strengthened Reinforced Concrete Curved Beams. International Conference on Civil Engineering and Applications.

Khalifa, A . and Nanni, A. (2002). Rehabilitation of rectangular simply supported RC beams with shear deficiencies using CFRP composites. *Construction and Building Materials*. 16, 135-146. doi:10.1016/S0950-0618(02)00002-8

Khalifa, A., Tumialan, G., Nanni, A. and Belarbi, A. (1999). Shear strengthening of continuous RC beams using externally bonded CFRP sheet. *American Concrete Institute, Proc., 4th International Symposium on FRP for Reinforcement of Concrete Structures (FRPRCS4)*, Baltimore, MD. 995-1008.

Khan, Asad Ur Rehman, and Shamsoon Fareed. (2014). Behavior of Reinforced Concrete Beams Strengthened By CFRP Wraps With And Without End Anchorages. *Procedia Engineering*. 77, 123-130.

Koutas, L., Triantafillou, T.C., 2012. Use of anchors in shear strengthening of reinforced concrete T-beams with FRP. Proceedings of the 6th International Conference on FRP Composites in Civil Engineering, CICE 2012.

Li, L., Guo, Y., Liu, F. and Bungey, J. (2006). An experimental and numerical study of the effect of thickness and length of CFRP on performance of repaired reinforced concrete beams. *Construction and Building Materials*. 20 (10), 901-909.

Mosley, B., Bungey, J. and Hulse, R. (2007). *Reinforced concrete design to Eurocode 2*, New York: Palgrave Macmillan.

Nanni, A., de Luca, A. and Zadeh, H., (2014). Reinforced Concrete with FRP Bars: Mechanics and Design. CRC Press: Taylor & Francis Group, Boca Raton, 23-35.

Nguyen-Minh, L. and Rovnák, M. (2015). Size effect in uncracked and precracked reinforced concrete beams shear-strengthened with composite jackets. *Composites Part B:Engineering*.78, 361-376. doi:10.1016/j.compositesb.2015.02.035

Obaidat, Y.T., Heyden, S., Dahlblom, O. and Abdel-Jawad Y. (2021). Retrofitting of reinforced concrete beams using composite laminates. *Construction and Building Materials*. 25, 591-597.

Pilkey, W.D. (2005). *Formulas for stress, strain and structural matrices,* New Jersey: John Wiley & Sons, Inc.

ProQuest, accessed 10 April 2021 http://www.proquest.com

Rafiq, Y.M.Y., Spearman, J. and Al-Farttoosi, M. (2015). Investigating the load carrying capacity of RC undamaged and damaged beams strengthened with CFRP. *Advances in Structural Engineering and Mechanics.*

Smith, S.T. and Teng, J.G. (2002). FRP-strengthened RC beams. *Review of debonding strength models. Engineering Structures*. 24 (4), 385-95.

Soliman, A.E.S. and Osman, M. (2012). Efficiency of using discrete fibers on the shear behaviour of R.C. beams, *Ain Shams Engineering Journal* (2012) 3, 209–217.

Sundarraja, M. and Rajamohan, S. (2009). Strengthening of RC beams in shear using GFRP inclined strips – An experimental study. *Construction and building materials*. 23, 856-864.

SubsTech 2012, accessed 2 April 2021 http://www.substech.com

Täljsten, B. (2003). Strengthening concrete beams for shear with CFRP sheets. *Construction and Building Materials*. 17 (1), 15-26.

Tamura, T. and Murata, H. (2010). Experimental study on the ultimate strength of R/C curved beam. *Proceedings of FraMCoS*-7, May 23-28, 2010.

Teng, J.G., Chen, J.F., Smith, S.T., 2001. Debonding Failures in FRP-Strengthened RC Beams: Failure Modes, Existing Research and Future Challenges. In: Composites in Construction: A Reality. Italy, pp. 139–148.

Thiagarajan and Ganesh. (2003). Experimental and Analytical Behavior of Carbon Fibre-Based Rods as Flexural Reinforcement. *Journal of Composites for Construction* - J COMPOS CONSTR. 7. doi:10.1061/(ASCE)1090-0268(2003)7:1(64)

Triantafillou, T.C., Antonopoulos, C.P., 2000. Design of Concrete Flexural Members Strengthened in Shear with FRP. *Journal of Composites for Construction* 4, 198–205.

Wisam H. K., Asala, A. D., Khattab S. A., Abdullah A. T. and Sultan N. A. (2021). Reinforced Concrete Curved Beams in Literature. *University of Diyala*.

Yazdani, N., Haque, F. and Hasan, I. (2016). Flexural and Shear Behavior of FRP Strengthened AASHTO Type Concrete Bridge Girders, *Journal of Engineering*, vol: 2016, 1-10. doi:10.1155/2016/5201910

Zhang, J., Chen, Z., Guo, X., 2016. Experimental Study on Fracture Behaviors of Concrete Beams Strengthened with FRP Sheet of Different Width. *International Journal of Materials Science and Applications* 5, 31.